

Tree Physiology 42, 229–252 https://doi.org/10.1093/treephys/tpab094



## Research paper

# Turgor-limited predictions of tree growth, height and metabolic scaling over tree lifespans

Aaron Potkay 1,4, Teemu Hölttä<sup>2</sup>, Anna T. Trugman<sup>3</sup> and Ying Fan<sup>1</sup>

<sup>1</sup>Department of Earth and Planetary Sciences, Rutgers University, New Brunswick, NJ 08854, USA; <sup>2</sup>Institute for Atmospheric and Earth System Research/Forest Sciences, University of Helsinki, Helsinki Fl-00014, Finland; <sup>3</sup>Department of Geography, University of California at Santa Barbara, Santa Barbara, CA 93106, USA; <sup>4</sup>Corresponding author (ajpotk@gmail.com)

Received March 2, 2021; accepted July 18, 2021; handling Editor Michael Ryan

Increasing evidence suggests that tree growth is sink-limited by environmental and internal controls rather than by carbon availability. However, the mechanisms underlying sink-limitations are not fully understood and thus not represented in large-scale vegetation models. We develop a simple, analytically solved, mechanistic, turgor-driven growth model (TDGM) and a phloem transport model (PTM) to explore the mechanics of phloem transport and evaluate three hypotheses. First, phloem transport must be explicitly considered to accurately predict turgor distributions and thus growth. Second, turgor-limitations can explain growth-scaling with size (metabolic scaling). Third, turgor can explain realistic growth rates and increments. We show that mechanistic, sink-limited growth schemes based on plant turgor limitations are feasible for large-scale model implementations with minimal computational demands. Our PTM predicted nearly uniform sugar concentrations along the phloem transport path regardless of phloem conductance, stem water potential gradients and the strength of sink-demands contrary to our first hypothesis, suggesting that phloem transport is not limited generally by phloem transport capacity per se but rather by carbon demand for growth and respiration. These results enabled TDGM implementation without explicit coupling to the PTM, further simplifying computation. We test the TDGM by comparing predictions of whole-tree growth rate to well-established observations (site indices) and allometric theory. Our simple TDGM predicts realistic tree heights, growth rates and metabolic scaling over decadal to centurial timescales, suggesting that tree growth is generally sink and turgor limited. Like observed trees, our TDGM captures tree-size- and resource-based deviations from the classical  $\frac{3}{4}$  power-law metabolic scaling for which turgor is responsible.

Keywords: hydraulic limitation, metabolic scaling, phloem transport, process-based model, turgor-driven expansion.

#### Introduction

Terrestrial carbon assimilated photosynthetically by vegetation and used for their growth is the weakest link in our understanding of the global carbon cycle (Ballantyne et al. 2015, Le Quéré et al. 2018) and predictions of its future (Friedlingstein 2015). These predictions come from dynamic global vegetation models (DGVMs) that often assume source-limited growth. Here, growth refers generally to net primary productivity and specifically to its component in the development of new structural biomass (rather than increases in non-structural storage), which allometrically involves increases in dimensions

(height, diameter, leaf area, etc.). By source-limitations, we mean that carbon assimilation limits growth and higher assimilation enhances growth in DGVMs (Fatichi et al. 2014). However, growing evidence suggests that growth is sink-limited, particularly cambial activity (Millard et al. 2007, Körner 2015), referring to environmental (temperature, water, nutrient) or internal (phloem-transport, cell-expansion, hormonal responses) controls on growth. The nuanced differentiation between sourceand sink-limitations becomes important when considering that future environmental stresses may slow and decouple growth from photosynthesis (Muller et al. 2011), potentially accumulating nonstructural carbohydrates (NSC) and raising

their concentrations (Körner 2003). Co-occurring elevated atmospheric  $CO_2$  concentrations stimulate growth, if only initially, and raise NSC concentrations (Dietze et al. 2014). Few DGVMs consider sink-limitations (Fatichi et al. 2014, Fatichi et al. 2019), and if they do, they often address environmental sink-limitations empirically (Leuzinger et al. 2013, Guillemot et al. 2017, Eckes-Shephard et al. 2021). Fewer include internal limitations such as NSC availability (Jones et al. 2019). Some have called for mechanistic, sink-driven modeling (Körner 2015, Fatichi et al. 2014, 2019, Friend et al. 2019) to capture growth and storage responses to environmental and physiological drivers.

Integrating ideas from more complex, mechanistic phloem transport models (PTMs; Thompson and Holbrook 2003a; Hölttä et al. 2006, Hölttä et al. 2009) and turgor-driven growth models (TDGMs; Génard et al. 2001; Steppe et al. 2006; De Schepper and Steppe 2010) offer a promising path toward understanding and predicting plant growth and carbon utilization. Both model classes simulate the roles of turgor in phloem transport (Münch 1930), cell expansion (Lockhart 1965) and division (Kirkham et al. 1972). Few models explicitly couple both phloem transport and turgor-driven growth (De Schepper and Steppe 2010, Hölttä et al. 2010), despite that phloemregulated, short-term osmotic changes may be considerable (Chan et al. 2016). These models and their underlying mechanisms are increasingly tested in laboratory and field experiments, capturing the sensitivity of trees' growth to NSC availability, water-stress and climate variability (Cabon, Fernández-de-Uña, et al. 2020, Cabon, Peters, et al. 2020, Hölttä et al. 2010, Peters et al. 2021). For instance, the turgor-driven mechanism underlying phloem transport (Münch 1930) has recently gained experimental support (Knoblauch et al. 2016, Savage et al. 2017) after nearly a century of experimental limitations (Knoblauch and Oparka 2012, Knoblauch and Peters 2017).

At least two matters should be resolved before mechanistic, sink-driven approaches can be applied in DGVMs. First, there are concerns that these models may be unsuitable for largescale application, due to their computational demand, complexity, large number of parameters and intensive calibration (Fatichi et al. 2014, Babst et al. 2018, Eckes-Shephard et al. 2021). Thus, integration requires development of mathematically simple and parsimonious yet mechanistically sound models, similar to the accomplishments for modeling photosynthesis (e.g., Farquhar et al. 1980). Cabon, Fernández-de-Uña, et al. (2020) and Cabon, Peters, et al. (2020) have recently shown that simplifications for TDGMs are indeed possible. Second, TDGMs are traditionally tested over durations shorter than a week (Steppe et al. 2006, De Schepper and Steppe 2010, Salomón et al. 2019) and recently over multiple years (Cabon, Fernández-de-Uña, et al. 2020, Cabon, Peters, et al. 2020, Coussement et al. 2020, Peters et al. 2021). Accordingly, these models require testing over longer timescales consistent

with those of global change prediction. Here, we develop a mathematically simple, mechanistic model of sink-limited growth appropriate for large-scale application. To demonstrate that the model predicts growth responses over decadal to centurial durations, we compare its predictions to measures of tree growth with consistent timescales to diagnose potential shortcomings. These measures include silvicultural site indices and metabolic scaling, against the latter of which few models are compared (e.g., Wolf et al. 2011).

Metabolic scaling refers to the allometric relationship between metabolic rates, particularly whole-plant growth rates (including stems, leaves and roots), G, and whole-plant biomass, C, and that  $G \propto C^{\beta}$ , which is often described by a  $^{3}/_{4}$  exponent ( $\beta = ^{3}/_{4}$ ; Niklas and Enquist 2001). Empirical values of  $\beta$  for trees, however, do not converge on  $\frac{3}{4}$  and may vary considerably among ecosystems (Price et al. 2009), declining under resource limitations and varying with tree-size (Muller-Landau et al. 2006, Russo et al. 2007, Coomes and Allen 2009). Indeed, tree rings initially grow wider with age or size in young trees, suggesting a positive value for  $\beta$ . However, past a critical age or size, older and larger trees grow gradually thinner annual rings (Cook et al. 1990, Fritts 1976), suggesting that  $\beta$  declines with tree age or size, approaching zero and later becoming negative. The ideal  $\frac{3}{4}$  scaling for plants has been theorized to result from the allometric scaling of xylem conductance (West et al. 1999, Sperry et al. 2012) and leaf area (Enquist and Niklas 2002). However, these theories assume that growth is proportional to photosynthetic carbon assimilation (Enquist et al. 1999) and thus postulates source rather than sink limitations, contrary to growing evidence (Körner 2015, Millard et al. 2007). Though growth and assimilation are coupled over annual or longer time-scales (von Allmen et al. 2012, Smith and Sperry 2014), the two become decoupled over shorter periods by environmental stress and variability due to the higher sensitivity of growth to reduced turgor from waterstress than to assimilation (Lempereur et al. 2015, Muller et al. 2011). Furthermore, assimilation itself may be sink-limited, since the utilization of photosynthates in sinks has to match the photosynthetic carbon assimilation rate, or carbohydrate accumulation will eventually force stomatal closure and downregulation of photosynthesis (Paul and Foyer 2001, Salmon et al. 2020). Hence, by predicting realistic metabolic scaling, our model may suggest a new, sink-limited perspective for metabolic scaling and may explain in part the variability in empirical  $\beta$ .

This study is guided by the following questions: How are growth predictions affected by considering sink-limitation? If proven important, can we parsimoniously build sink-driven growth for DGVMs through principles of phloem-transport and turgor-driven growth? Can turgor-driven mechanisms explain decadal to centurial tree growth phenomena, particularly their height-age and growth-size scaling, including the metabolic

scaling exponent,  $\beta$ , and its behavior? We answer these questions by designing a new, mechanistic sink-limited growth model involving a PTM and a TDGM. We compare model behavior to well-recognized tree-growth trends (site indices and metabolic scaling) and source-limited modeling schemes. We test three hypotheses. First, axial phloem transport must be considered explicitly to accurately predict turgor distributions with changing water availability and plant hydraulic strategy and thus to predict growth. Second, turgor-driven growth can explain growth-scaling of trees, both theorized (West et al. 1999, Enquist and Niklas 2002) and observed (Muller-Landau et al. 2006, Coomes and Allen 2009, Smith and Sperry 2014). Following this second hypothesis, we expect turgor dynamics will control variations in  $\beta$  due to turgor changes from treesize (Woodruff et al. 2004, Woodruff and Meinzer 2011) and external water-stress (Sevanto 2014, Salmon et al. 2019). However, this second hypothesis considers allometric scaling (i.e.,  $\beta$ ) but not actual growth rates. Thus, third, we hypothesize that turgor-driven growth explains decadal growth rates and height-age trends. We test our second and third hypotheses through both, in a technical sense, offline and online simulations, in which TDGM simulations are conducted using prescribed and simulated model inputs, respectively. In offline simulations, we feed the TDGM with inputs taken from past, literature-reported data, and in online simulations, we couple the TDGM to a dynamic tree growth model (THORP; Potkay et al. 2021). Online simulations allow the two-way interaction between our TDGM and THORP, while offline simulations isolate the TDGM response to static environmental conditions. Online predictions of height are compared with site indices of Scots Pine trees in forest stands of Northern Spain (Tillar Valley; Poblet Forest Natural Reserve; Prades Mountains) (Bravo and Montero 2001, Palahi et al. 2004), where Potkay et al.'s (2021) original THORP simulations were based. In sum, we hypothesize that sinklimited growth is consistent with well-established tree growth phenomena that are traditionally understood through sourcelimitations, including tree height-age trends (e.g., Mäkelä 1985, King 1990) and metabolic scaling (West et al. 1999, Enquist and Niklas 2002, Sperry et al. 2012).

## Methods

We develop a steady-state, whole-tree PTM (see Notes S1; Section S.1 available as Supplementary data at *Tree Physiology* Online) and a whole-stem TDGM (see Notes S1; Section S.2 available as Supplementary data at *Tree Physiology* Online). TDGMs are often tested assuming either constant osmotic potential (Cabon, Peters, et al. 2020) or osmotic dilution of a constant quantity of solutes in an expanding volume (Cabon, Fernández-de-Uña, et al. 2020). These simplistic assumptions may be appropriate over short timescales when osmotic changes are small; however,

significant osmotic changes have been observed over diurnal (Chan et al. 2016, Lazzarin et al. 2019) and seasonal (Simard et al. 2013) timescales. We expect that changes in osmotic potentials become more important over longer timescales such as during periods of water-stress and as tree-size changes become significant (Woodruff 2014; Epron et al. 2019) in accord with our first hypothesis that phloem transport must be explicitly considered to predict turgor-driven growth. Thus, our original intent was to couple these two models where the sinkdemand from the TDGM would inform the PTM, and the turgor distribution from the PTM would inform the TDGM. However, we found that it was not necessary to explicitly predict turgor distributions by the PTM, contrary to our first hypothesis, and osmotic potentials can be assumed uniform at least as a firstorder approximation (see Results; Figure 2). Thus, we do not couple the two modules in the final version of the TDGM. We perform offline and online simulations of the TDGM. In offline simulations, we feed the TDGM with inputs taken from past, literature-reported data, and its predictions reflect solely sinklimitations, since photosynthesis and source-limitations are not considered here. Offline simulations were performed to explore the TDGM's predictions of  $\beta$  and to test our second hypothesis that turgor explains metabolic scaling of trees. These offline simulations predict growth for a given tree-size, particularly the scaling between size and growth rate, but they cannot say for how long or at what age any stem biomass is reached. Thus, we also perform online simulations to predict dynamic responses to test our third hypothesis that turgor can explain realistic tree growth-age trends. We perform online simulations, which consider both source- and sink-dynamics, by coupling our TDGM with a numerical, process-based, individual tree model, the Tree Hydraulics and Optimal Recourse Partitioning model (THORP; Potkay et al. 2021). The coupling of THORP and our TDGM is summarized below and fully detailed in the Supplementary data (see Notes S1; Section S.3 available as Supplementary data at Tree Physiology Online). All codes for models and analyses are included in the Supplementary data (see Notes S2 available as Supplementary data at Tree Physiology Online).

Generally, we present and discuss results from our online and offline TDGM simulations in terms of whole-tree growth rates in C equivalents [(mol C)•s<sup>-1</sup>] (e.g., Figures 3a and 7a–c), including growth occurring both above- and below-ground as well as both radial and axial stem growth. Predictions of tree age versus height are compared against height measurements (site indices) (Figures 5 and 6); nonetheless, this presentation also implies a consideration of the whole-tree, since THORP consider the co-occurring leaf, root and radial stem growth required to metabolically, hydraulically and structurally support increases in height. Additionally, we also consider growth in terms of annual, whole-tree C increments in online simulations (Figure 7d–f). Below we briefly describe the PTM and TDGM. All mathematical

symbols are defined in Table S1 available as Supplementary data at *Tree Physiology* Online.

#### Phloem transport model

We present a 1D, steady-state PTM for the partitioning of sugar between shoot and root for respiration and growth (see Section S.1 available as Supplementary data at *Tree Physiology* Online). Our PTM is inspired by early transport-resistance models (Dewar 1993, Thornley 1972), which predict plant growth and allocation from simple representations of phloem transport. Our PTM is an inversion of transport-resistance models, and we estimate steady-state phloem transport from known metabolic demands and allocation for a tree with realistic branching architecture (Figure 1a). Though some PTMs explicitly resolve phloem transport among complex branching architectures (e.g., Nikinmaa et al. 2014), we circumvent this challenge by collapsing branches into an equivalent, 1D column (Figure 1b), an approach applied in past studies of allometric scaling (West et al. 1999, Sperry et al. 2012, Hölttä et al. 2013). Notable assumptions and simplifications include:

- (i) all phloem sap osmolytes behave like sucrose,
- (ii) xylem-phloem coupling enables water-potential equilibrium (Daudet et al. 2002, Hölttä et al. 2006, Thompson and Holbrook 2003b),
- (iii) water potentials vary linearly along the stem axis,
- (iv) phloem sap viscosity is uniform along the stem axis,
- (v) Da Vinci's rule for area-preserving branching (Figure 1b; von Allmen et al. 2012; Bentley et al. 2013) and pipe model theory (Shinozaki et al. 1964), suggesting carbon demands for stem and leaf growth are approximately uniform (Figure 1c),
- (vi) stem diameter, phloem thickness and phloem conductance are non-uniform and follow power-law allometries (Figure 1b; Hölttä et al. 2013; Savage et al. 2017; Clerx et al. 2020),
- (vii) stem respiration is non-uniform and proportional to phloem area and
- (viii) phloem loading is not source-limited, equals sink demand in steady-state (alternatively, phloem unloading is sink-limited; Patrick 2013) and is distributed exponentially within the canopy (Figure 1c).

These assumptions are fully discussed and justified in the PTM description (see Notes S1; Section S.1 available as Supplementary data at *Tree Physiology* Online), and from them, we estimate how phloem loading and unloading are distributed between stem apex and root collar (Figure 1c; see Notes S1, Section S.1.1 available as Supplementary data at *Tree Physiology* Online). Notably, sugar is unloaded along the phloemtransport path within the stem to support stem respiration,  $R_S$  [(mol C)•s<sup>-1</sup>], and the sum of aboveground growth and construction respiration,  $(1-u_R) \cdot G/(1-f_c)$ , where  $u_R$  is the

carbon allocation fraction to root-growth, *G* is whole-tree growth [(mol C) $\bullet$ s<sup>-1</sup>] and  $f_c$  accounts for the proportionality between growth and construction respiration (0  $\leq f_c <$  1). From phloem loading and unloading, we estimate how phloem sugar fluxes are distributed (Figure 1d; see Notes S1; Section S.1.2 available as Supplementary data at Tree Physiology Online). This downward sugar flux from stem apex to roots satisfies belowground sink demands: maintenance respiration,  $R_R$  [(mol C) $\bullet$ s<sup>-1</sup>], and the sum of consumption for growth and construction respiration,  $u_R \cdot G/(1-f_c)$ . This sugar flux is driven by osmotically generated pressure gradients between sources and sinks (Münch 1930), resulting from higher sugar concentration and turgor in sources and lower concentrations and turgor in sinks where sugar unloading and consumption occurs. Thus, we estimate sugar concentrations from the estimated sugar fluxes (Figure 1e; see Notes S1; Section S.1.3 available as Supplementary data at Tree Physiology Online).

The solution for phloem sugar concentration,  $c_p$ , as a function of distance from stem apex, z, is derived in the Supplementary data (see Section S.1 available as Supplementary data at *Tree Physiology* Online) and defined by two dimensionless terms. Distance is normalized by the tree height,  $\tilde{z}=z/H$ . Sugar concentration is described by a dimensionless form of Seleznyova and Hanan's (2017, 2018) carbon potential,  $\Phi = (c_p/c_{p,S})^2$ , where  $c_{p,S}$  is the phloem sugar concentration at the stem apex.

$$\overset{\sim}{\Phi} = \exp\left(\frac{\eta - \theta}{\varepsilon} \overset{\sim}{z}\right) \left[\frac{\eta - 2\theta}{\eta - \theta} - \frac{\zeta}{\varepsilon}\Theta\right] + \frac{\theta}{\eta - \theta}.$$
 (1)

Equation 1 (same as see Eq. S.1.36 available as Supplementary data at Tree Physiology Online) is defined by three constants with units of [MPa $\bullet$ (mol sucrose) $\bullet$ m<sup>-4</sup>],  $\theta$ ,  $\eta$  and  $\varepsilon$  (see Eq. S.1.32-34 available as Supplementary data at *Tree Physiology* Online).  $\theta$  represents the advection due to gravity and water potential gradients,  $\psi'$ , and thus further reflects xylem sap flow, transpiration and water-stress (Venturas et al. 2017).  $\eta$ represents the sugar flow driven by phloem sap density-induced buoyancy, and  $\ensuremath{\varepsilon}$  represents the coordination between phloem sugar concentrations and osmotic potentials (i.e., the van't Hoff formula or nonlinear equivalents), further diminished by treesize. A fourth constant,  $\zeta$ , has units of hydraulic resistance [MPa•s•m<sup>-4</sup>] and represents the maximum phloem conductance, including the viscosity affects (see Eq. S.1.35 available as Supplementary data at Tree Physiology Online).  $\Theta$  is a function of  $\tilde{z}$  and shares units with the phloem sap flux, i [(mol sucrose) •s<sup>-1</sup>]

$$\Theta = \int \exp\left(\frac{\theta - \eta}{\varepsilon} \widetilde{z}\right) \widetilde{z}^{-\delta} j \, d\widetilde{z}, \tag{2}$$

where j depends on  $\tilde{z}$  according to sink demands (growth and respiration; see Eq. S.1.21 available as Supplementary data

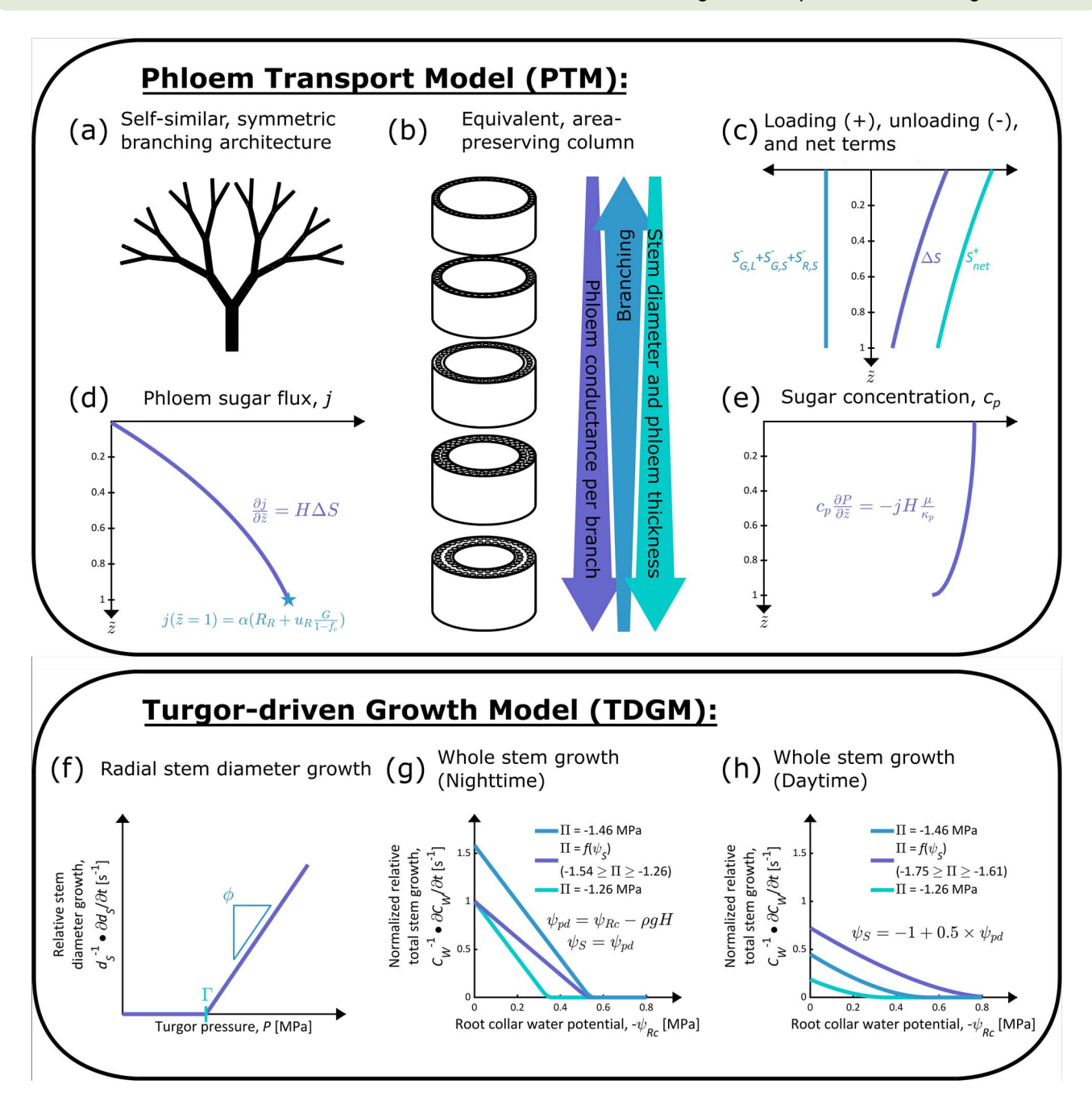


Figure 1. Schematic of PTM (a-e) and whole-tree TDGM (f-h). The PTM describes the turgor-gradient driven flow of sugars through a self-similar, symmetric stem branching architecture (a), which is solved by collapsing all branches into an equivalent column with conserved stem cross-sectional area and heterogeneous phloem properties (b). Column cross-sections show phloem architecture. From stem architecture and structure (e.g., Da Vinci's rule, pipe model theory; a and b), we estimate how phloem loading  $(S_{net}^+)$ , unloading for leaf growth and leaf construction respiration  $(S_{G,L}^-)$ , stem growth and stem construction respiration  $(S_{G,S}^-)$ , and stem respiration  $(S_{R,S}^-)$ , and their sum  $(\Delta S)$  are distributed from stem apex  $(\tilde{z}=0)$  to root collar ( $\tilde{z} = 1$ ) (c). From  $\Delta S$  (c), we estimate how phloem sugar fluxes (j) in steady-state are distributed (d). The sugar flux at the root collar (blue star) satisfies root maintenance respiration  $(R_R)$ , root growth and root construction respiration  $(u_R \cdot G/(1-f_c))$ . From j (d), we estimate how sugar concentrations,  $c_P$ , are distributed (e). Additional PTM variables in (a–e) include tree height (H), a molar conversion factor from C to sugars ( $\alpha$ ), turgor pressure (P), viscosity  $(\mu)$  and phloem permeability  $(\kappa_p)$ . The TDGM describes turgor-limited, whole-tree growth for a tree with a self-similar, symmetric stem branching architecture (a). For each individual branch with diameter ( $d_S$ ), radial growth occurs once P exceeds a threshold ( $\Gamma$ ) (f). For  $P > \Gamma$ , relative stem diameter growth rates  $(d_S^{-1} \bullet \partial d_S / \partial t)$  increase with P by the extensibility  $(\phi)$ . We show TDGM predictions for nighttime (g)and daytime (h), which depend on root collar water potentials ( $\psi_{RC}$ ), stem apex water potentials ( $\psi_S$ ), osmotic potentials ( $\Pi$ ) and turgor threshold  $(\Gamma = 0.9 \text{ MPa})$ . The x-axis in (g and h) is a proxy for soil water-stress. Estimates are shown for a 4.4-m-tall tree with either constant  $\Pi = -1.46 \text{ MPa}$ 

at *Tree Physiology* Online), and  $\delta$  defines how phloem conductance vary along the stem axis (see Eq. S.1.30 available as Supplementary data at *Tree Physiology* Online). The full equation for  $\Theta$  is given by Eq. S.1.38 available as Supplementary data at *Tree Physiology* Online.

## Turgor-driven growth model

We present a simple model of stem growth,  $\partial C_W/\partial t$  (S.2 in SI), where  $C_W$  is stem biomass, expressed here in molar C equivalents [mol C]. Our TDGM describes the growth of the entire stem, including radial and axial growth and changes in tree architecture and branching. Like our PTM, we assume:

- (i) xylem-phloem water-potential equilibrium,
- (ii) Da Vinci's rule and
- (iii) stem diameter,  $d_S$ , and phloem thickness,  $d_p$ , follow power-law allometries  $(d_p \propto d_S^b)$ .

#### Additionally, we assume:

- (i) height, H, and basal stem diameter, D, follow allometric power-law scaling ( $D \propto H^{\circ}$ ; McMahon 1973; Niklas and Spatz 2004),
- (ii) stem biomass,  $C_W$ , is proportional to  $H \bullet D^2$  (Buckley and Roberts 2006, Mäkelä 1986),
- (iii) the Lockhart (1965) equation for turgor-driven cell expansion successfully describes organ level growth (Figure 1f; Génard et al. 2001, Steppe et al. 2006) and
- (iv) stem growth is related to whole-tree growth, G, through a dimensionless stem allocation fraction,  $u_S$   $(\partial C_W/\partial t = u_S \bullet G)$ .

These assumptions are fully discussed in the TDGM description (see Notes S1; Section S.2 available as Supplementary data at *Tree Physiology* Online). The final equation for *G* is given by the expression (equivalent to Eq. S.2.13 available as Supplementary data at *Tree Physiology* Online)

$$G = \frac{1 + 2a}{ab} \phi \frac{C_W}{u_S} \int_0^1 \max(P - \Gamma, 0) \ d\widetilde{z}, \tag{3}$$

where a is a scaling exponent between height and basal diameter [-] ( $a \approx 1.5$  according to elastic similarity and Euler buckling; McMahon 1973; Niklas and Spatz 2004), b is a scaling exponent between phloem thickness and stem diameter [-] ( $0 < b \le 1$ ; see range in Table 1), P is  $\tilde{z}$ -dependent turgor pressure [MPa] and  $\phi$  and  $\Gamma$  are parameters from the Lockhart (1965) equation.  $\phi$  is the extensibility [MPa $^{-1} \bullet s^{-1}$ ], and  $\Gamma$  is the threshold turgor [MPa]. Traditionally, the symbol,  $\phi$ , represents

the extensibility of an individual cell (Lockhart 1965); however,  $\phi$  here refers the bulk extensibility of bulk stem tissue as often applied in some TDGMs (Génard et al. 2001, Steppe et al. 2006). Preliminary versions of the TDGM were coupled to the PTM (Eq. 1) to calculate  $P(\tilde{z})$  from  $c_p(\tilde{z})$  (likewise G from Eq. 3 was fed into the calculation of phloem fluxes through Eq. S.1.19 available as Supplementary data at  $Tree\ Physiology\ Online$ ); however, the coupling was later deemed unnecessary, since  $c_p$  was found to be nearly uniform regardless of parameterization (see Results; Figure 2).

Thus, given uniform osmotic potentials,  $\Pi$  [MPa] due to uniform  $c_p$ , and further assuming a linear water potential variation across the stem axis, Eq. 3 simplifies to our final closed-form solution

$$G = \frac{1+2a}{ab}\phi \frac{C_W}{u_S}$$

$$\left[ (\psi_S - \Pi - \Gamma) \left( 1 - \overset{\sim}{z}^+ \right) + \frac{\psi_{Rc} - \psi_S}{2} \left( 1 - \overset{\sim}{z}^{+2} \right) \right], \quad (4)$$

where  $\psi_S$  and  $\psi_{Rc}$  are the water potentials at the stem apex and root collar, respectively [MPa], and control the TDGM's response to water-stress (Figure 1g and h), and  $\tilde{z}^+$  denotes where along the stem axis  $P=\Gamma$ , further bound by the limits of  $\tilde{z}$  (0  $\leq$   $\tilde{z}^+ \leq$  1).

$$\tilde{z}^{+} = \min \left[ \max \left( \frac{\Pi + \Gamma - \psi_{S}}{\psi_{RC} - \psi_{S}}, 0 \right), 1 \right]. \tag{5}$$

How osmotic potentials respond to water-stress further modulate the TDGM (Figure 1g and h). When applying Eq. 4 here, osmotic potentials are simply modeled from  $\psi_S$ . First, phloem sap molality,  $m_p$  [mol $\bullet$ kg $^{-1}$ ], was predicted according to regressions for Scots Pine ( $m_p = 0.48-0.13 \bullet \psi_S$ ; Paljakka et al. 2017). Then, we calculated  $\Pi$  from  $m_p$  by the equations in Thompson and Holbrook (2003a; their Eqs 9 and 10), assuming sap osmolytes behave like sucrose. This simplistic approach captures basic osmotic regulation, but it does not consider the possibility of more complex behaviors for drought-induced osmotic adjustment such as the nuances between rapid drying and gradual acclimation (Jones and Turner 1978). However, osmotic adjustments due to drought acclimation are generally small relative to pre-drought osmotic potentials (Bartlett et al. 2014), and osmotic potentials from control and droughted conifers are similar (Paljakka et al. 2017; Salmon et al. 2020; see Figure S1 available as Supplementary data at Tree Physiology Online), suggesting that the rapid component of osmotic adjustment is sufficient for our TDGM.

(blue line), constant  $\Pi=-1.26$  MPa (green line) or osmotic regulation (purple line), where  $\Pi$  is positively-related to  $\psi_S$  according to Paljakka et al. (2017), and all growth rates are normalized by the maximum nighttime growth rate with osmotic regulation (purple line in g). For nighttime growth estimates (g),  $\psi_S$  here equals the predawn water potential ( $\psi_{pd}=\psi_{Rc}-\rho gH$ ). For daytime growth estimates (h),  $\psi_S$  here equals  $-1+0.5\times\psi_{pd}$ , based on Martínez-Vilalta et al. (2014). Additional TDGM variables in (f-h) include the density of water ( $\rho$ ) and the acceleration due to gravity (g).

Downloaded from https://academic.oup.com/treephys/article/42/2/229/6325580 by University of Illinois at Urbana-Champaign user on 25 June 2022

alysis
n ani
tatio
permu
atic
systen
.⊆
values
tested
ind t
nifer a
II con
n-tall
4.4-r
for
puts
.⊑ ∑
d PT
esize
Synthe
ώ,
Table 1

Symbol	Meaning	Representative value	Units	Reference	Tested values
Cp,S	Phloem sap sugar concentration at stem apex	009	(mol suc) •m <sup>-3</sup>	Jensen et al. (2013)	100, 600, 1200,
μ	Phloem sap viscosity	*2•10-9	MPa∙s	Bouchard and Graniean (1995)	*2•10-9
ks	Constant relating sap sugar concentration to osmotic potential	-	1	Hall and Minchin (2013)	1, 2
κ <sub>ρ,0</sub>	Phloem permeability at base of trunk for reference tree height, $\hbar$	2•10 <sup>-16</sup>	m <sup>4</sup>	Epron et al. (2019)	$2 \bullet 10^{-14}, 2 \bullet 10^{-16},$ $2 \bullet 10^{-18}$
h	Reference height	ന	٤		æ
<u> </u>	Exponent describing how permeability scales with tree height <sup>†</sup>	2.5	1	Hölttä et al. (2013), Jyske and Hölttä (2015), Knoblauch et al. (2016), Savage et al. (2017), Liesche et al. (2017), Epron et al. (2019), Losada and Holbrook (2019), Clerx et al. (2020)	1.5, 2.5, 3.5
8	Exponent describing how permeability scales	-0.5	I		-1.5, -0.5, 0.5
	along the stem axis				
Ø	Exponent describing scaling between distance and stem diameter	1.5	I	Niklas and Spatz (2004), Hölttä et al. (2013), Mäkelä et al. (2019)	1, 1.5
q	Exponent describing scaling between stem diameter and phloem thickness	2/3	1	Génard et al. (2001), Steppe et al. (2006), Hölttä et al. (2013), Rosell (2016), Rosell et al. (2017), Salomón et al. (2019)	0, <sup>1</sup> / <sub>5</sub> , <sup>2</sup> / <sub>5</sub> , 1
Rs	Stem maintenance respiration rate	**2,6 <b>•</b> 10 <sup>-11</sup>	(mol C) •s <sup>-1</sup>	Poorter et al. (2012), Schiestl-Aalto et al., (2015), Potkay et al. (2021)	** 2.6•10 <sup>-13</sup> , ** 2.6•10 <sup>-12</sup> , ** 2.6•10 <sup>-11</sup> , ** 2.6•10 <sup>-11</sup> , ** 2.6•10 <sup>-10</sup> ,
$R_{R}$	Root maintenance respiration rate	**5.8•10 <sup>-8</sup>	(mol C)•s <sup>-1</sup>		**5.8 10 <sup>-10</sup> , **5.8 10 <sup>-10</sup> ,
					**5.8•10 <sup>-8</sup> ; **5.8•10 <sup>-7</sup> ; **5.8•10 <sup>-7</sup> ;
, ,	Water potential gradient	0.015	MPa∙m <sup>-1</sup>	Woodruff et al. (2004), Woodruff and Meinzer (2011)	0.010, 0.012,
					(Continued)

Table 1. Continued

Symbol	Meaning	Representative value	Units	Reference	Tested values
$f_c$	Proportionality between growth and construction respiration rates	0.28	I	Chung and Barnes (1977)	0.28
9	Whole-tree growth rate	2•10 <sup>-7</sup>	(mol C)•s <sup>-1</sup>	Potkay et al. (2021)	2•10 <sup>-9</sup> , 2•10 <sup>-8</sup> , 2•10 <sup>-7</sup> , 2•10 <sup>-6</sup> , 2•10 <sup>-5</sup>
u <sub>R</sub>	Fraction of growth occurring in roots Coefficient describing how phloem loading rates are distributed along the stem	6.0	1 1	De Pury and Farquhar (1997),	0.2, 0.5, 0.8
7	Temperature	298.15	×	Mencuccini and Grace (1996)	0.56, 5.6 283.15, 298.15, 313.15

\*Value reported as general value for phloem sap viscosity. In analysis,  $\mu$  was made both temperature- and sugar concentration-dependent according to the equations by Bouchard and Granjean (1995), using  $c_{
ho,S}$  as the sugar concentration governing  $\mu_{
m c}$ 

\*\*\*Value of zero for  $\sigma$  represents uniformly distributed net loading. However, setting  $\sigma$  equal to zero is not solvable by the current model formulation (e.g., division by terms like  $1 - \exp(-\sigma)$ ), \*\*Value reported at 25 °C, and made temperature-dependent in analysis by a Q10 formulation according to equations in Potkay et al. (2021) and consequently,  $\sigma$  was set to  $10^{-10}$  in this case.

 $^{\dagger}\lambda$  describes the scaling of phloem permeability at base of trunk with tree height,  $\kappa_{\rho}(\tilde{z}=1) \propto H^{\lambda}$ . Values for  $\lambda$  are estimated by first rewriting  $\kappa_{\rho}(\tilde{z}=1) = \kappa_{i}(\tilde{z}=1) \bullet \bullet \iota_{i}(\tilde{z}=1)$ , where  $\kappa_{i}$  is the permeability of individual phloem sieve elements, including end wall resistances, and  $n_i$  is the number of phloem sieve elements.  $\kappa_i$  is related to H by a power-law with an exponent that we estimated from past literature with values including ~0.3 for a non-woody vine (Knoblauch et al. 2016), ~1 for angiosperm and gymnosperm trees (Liesche et al. 2017, Savage et al. 2017) and ~1.5 for a woody, angiosperm shrub and Red Oak (Clerx et al. 2020, Losada and Holbrook 2019). ni is related to stem diameter at breast height, D, by a power-law with an exponent that we estimated from past literature with values including ~1 (Clerx et al. 2020; a similar value is reached when combining power-law allometries of phloem conduit density and phloem area; Hölttä et al. 2013; Jyske and Hölttä 2015) and ~1.5 (Epron et al. 2019). From these power-law allometries for  $\kappa_i$  and  $n_i$ , and assuming  $D \propto H^{15}$  (Niklas and Spatz 2004), we estimated our best guess for λ and the limits of its range.

the describes the scaling of phloem permeability with distance from stem apex,  $\kappa_{\rho} \propto z^{-\delta}$ . Values for δ are estimated by first rewriting  $\kappa_{\rho} = \kappa_{r} \bullet n_{r} \bullet N$ , where N is the furcation number or number of branches. Given our PTM's assumption of Da Vinci's rule, we find  $N \propto \tilde{z}^{-2\sigma}$  (Eq. S.1.14), and thus  $\delta = \lambda - 2a$ .  $\delta < 1$  for real solutions.

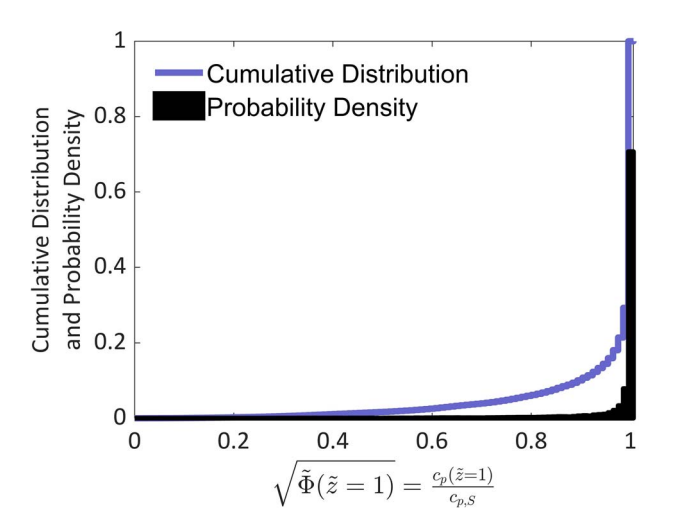


Figure 2. Cumulative distribution and probability density distribution of more than  $1.76 \bullet 10^9$  predictions of the PTM given different combination of inputs for a 4.4-m-tall conifer (Table 1). The *x*-axis represents the ratio between the sugar concentrations at the stem apex and root collar,  $c_p(\tilde{z}=1)/c_{p,S}$ ; thus, a value of unity suggests uniform sugar concentrations along the phloem pathway.

#### Systematic permutation of PTM

To test our first hypothesis that phloem transport must be considered explicitly to accurately predict turgor distributions and thus turgor-driven growth, we perform a systematic permutation analysis of our PTM's predictions of sugar concentration in steady-state when sink-limited. To explore the PTM's sensitivity to inputs, we test all possible combinations of plausible values of inputs and report the sugar concentration ratio of the root collar ( $\tilde{z} = 1$ ) to the stem apex ( $\tilde{z} = 0$ ), denoted simply by  $\Phi(\tilde{z}=1)$ . We synthesized reasonable values for the inputs for a 4.4-m-tall conifer from the literature and chose ranges to test, often varying inputs over several orders of magnitude to reflect the lack of sufficient knowledge to accurately constrain observed values (Table 1). A height of 4.4 m was chosen to be tall enough to clearly meet our PTM's assumption that stem area is conserved across furcation (i.e., Da Vinci's rule; Bentley et al. 2013); however, trees slightly shorter by a meter or two may also meet this prerequisite (von Allmen et al. 2012). Overall, we test more than 1.76•109 combinations of inputs. We do not present predictions of sugar concentration that are negative, complex solutions, imaginary numbers or would result in the maximum possible turgor at the stem apex being negative (i.e., the solutions for which  $\psi(\tilde{z}=0) < \Pi(\tilde{z}=0)$ , assuming  $\psi(\tilde{z}=0)$ 1) is negligible). We repeat this analysis for a larger, 44-m-tall conifer, testing different combinations of inputs reflecting larger tree-size (see Table S2 available as Supplementary data at Tree Physiology Online). Here, a height of 44 m was chosen to be an order of magnitude taller than the tree in our other permutation analysis and because few conifers grow taller than this height (Tao et al. 2016).

We recognize that exponents related to how phloem conductance scales within a tree and with tree size ( $\delta$  &  $\lambda$  in Table 1) were taken from studies of various plant types and sizes, despite their differences in sieve element anatomy (Liesche et al. 2017). For this reason, we tested our PTM to a wide range of these exponents (Table 1). Unlike our TDGM, in which osmotic potentials (and thus sugar concentrations) are modeled from stem water potentials ( $\psi_S$ ), we test the PTM with multiple values of stem apex sugar concentrations (Table 1). We made this choice to test the PTM to the natural range of phloem sap sugar concentrations (Jensen et al. 2013) and because the PTM does not explicitly represent the magnitude of water potentials (e.g.,  $\psi_S$ ). Nonetheless, our PTM includes the gradient in water potentials across the stem,  $\psi'$ , to calculate the gradient in turgor that drives phloem transport (Münch 1930).

#### Offline simulations of TDGM

We test our second hypothesis from the TDGM's predictions of metabolic scaling by performing offline simulations of Eq. 4 over nine orders of magnitude of total tree biomass. Total biomass, C, was calculated from stem biomass,  $C_W$ , applying Poorter et al.'s (2012) regression for stem mass fraction, SMF, with plant size (see Figure S2 available as Supplementary data at *Tree Physiology* Online;  $C = C_W \bullet \text{SMF}^{-1}$ ). Height was calculated by the equations used by Potkay et al. (2021; same as in TDGM) and their parameters for Scots Pine. Analyses are limited to trees taller than 1 m, since some of the TDGM's assumptions (Da Vinci's rule; allometric scaling) collapse at small statures (Niklas and Spatz 2004, von Allmen et al. 2012).

Stem allocation fraction,  $u_S$ , is age- and size-dependent (Potkay et al. 2021, Xia et al. 2019), and we apply previously predicted values of  $u_S$  from THORP (Potkay et al. 2021; their well-watered, control simulation), and we regressed  $u_S$  as a function of height (see Figure S3 available as Supplementary data at Tree Physiology Online). Similar to u<sub>S</sub>, we apply previously predicted, height-dependent water potentials,  $\psi_S$  and  $\psi_{Rc}$ , from THORP in offline simulations. These predictions of  $\psi_S$  and  $\psi_{Rc}$  for a given tree-size include the gravitational effect of height, the size-dependent scaling stem xylem conductance (Sperry et al. 2012, West et al. 1999) and transpiration, thereby depending on stomatal control and xylem conductance of leaves and roots. Potkay et al. (2021) ran THORP with realistic atmospheric conditions from NOAA reanalysis data (NCEP/NCAR Reanalysis 1; Kalnay et al. 1996) with both inter- and intraannual variability, repeating 10-year forcing over more than a century to simulate a stable climate, and thus, the resulting  $u_S$ and water potentials oscillated at these timescales (see Figures S3 and S4 available as Supplementary data at Tree Physiology Online). Since most growth will occur when turgor is largest, we apply THORP's predicted water potentials at their least negative values for a given tree-size (upper 95% confidence limit; see Figure S4 available as Supplementary data at Tree Physiology

Online), coinciding with the wettest periods from the repeated forcing data. We present offline TDGM results applying predawn water potentials (see Figure S4a available as Supplementary data at *Tree Physiology* Online), coinciding with when most growth has been hypothesized to occur (Steppe et al. 2015) and has been recently observed (Zweifel et al. 2021). However, we also test the model with growth predicted from midday water potentials (see Figure S4b available as Supplementary data at *Tree Physiology* Online) and with growth equal to the arithmetic mean of predawn and midday growth rates.

In offline simulations, the values of a, b and extensibility,  $\phi$ , were arbitrarily chosen, since these constants do not affect the predicted  $\beta$ . The model is, however, sensitive to the turgor threshold,  $\Gamma$ , for which we present results at multiple values.

#### Online simulations of TDGM

While offline simulations consider allometric scaling (i.e.,  $\beta$ ), they do not explicitly consider age or time and thus do not guarantee the magnitudes of actual growth rates. Thus, to test our third hypothesis that including turgor-driven growth can better predict growth rates and height-age trends, we perform online, dynamic simulations with a numerical, individual tree model and corroborate results from our offline simulations. We developed THORP-G, a modified version of THORP that predicts growth rates according to the TDGM (Eq. 4), and rerun Potkay et al.'s (2021) well-watered, control simulation with the new scheme capable of capturing sink- and turgor-limited growth.

As detailed by Potkay et al. (2021), THORP predicts growth and the dynamic growth allocation fractions at subdaily timesteps that reflect environmental conditions by optimizing tree productivity. THORP's optimization considers the benefits associated with investing in its hydraulic architecture and ability to intercept light. It has been shown to capture realistic allometric changes due to size and various environmental stimuli. THORP's allometric optimization balances the internal tree resistances across roots, stems and leaves, and thus, THORP explicitly simulates xylem hydraulics similar to Sperry et al. (1998). Stomatal conductance are predicted by a modified version of Sperry et al.'s (2017) Gain-Cost stomatal optimization, which differs slightly from the original Gain-Cost algorithm. Potkay et al. (2021) equated leaf temperatures with air temperatures and modified the belowground conductance of the soil-root pathway to explicitly account for the vertical distribution of roots mass. The Gain-Cost optimization algorithm has been validated at the individual plant level in garden experiments (Venturas et al. 2018, Wang et al. 2019, Wang et al. 2020) and ecosystem level (Sabot et al. 2020, Venturas et al. 2020). Belowground and leaf conductances are proportional to root and leaf biomasses, respectively, and stem conductance is nonlinearly dependent on tree-size according to a fractal-like hydraulic tree architecture and sapwood-heartwood proportions (Hölttä et al. 2013, Savage et al. 2010, Sperry et al. 2012,

West et al. 1999). The hydraulic limitations of height (Ryan and Yoder 1997) are represented by THORP. THORP's water potential predictions have been validated against observations (Potkay et al. 2021). Additionally, THORP simulates light interception, photosynthetic carbon assimilation (Farguhar et al. 1980, Sperry et al. 2017) and soil hydrology from atmospheric forcing at subdaily time-steps. We refer to this new version of THORP coupled to the TDGM as THORP-Growth or simply THORP-G. It is noteworthy that THORP predicts the allocation among organs that optimizes carbon assimilation, suggesting a source-limitation to growth; however, THORP-G now includes the possibility of sink-limitations. When assimilation exceeds metabolic demands, NSC storage increases, and the excess may be used later to support future metabolic demands when assimilation is low. Nevertheless, optimizing carbon assimilation is a valid strategy for competition, survival and fitness, whether the assimilated carbon is used to support current growth or as storage to support future sink demands.

The original, uncoupled version of THORP included a single carbon storage pool and assumed growth rates proportional to the storage size (Potkay et al. 2021); however, this past representation reduces to a source-limited perspective of growth when considered in steady-state. Thus, comparison of THORP and THORP-G reveals potential differences between source- and sink-limited schemes. While growth predictions from THORP-G largely reflect sink-limitations, source-limitations are not completely ignored in these online simulations, and growth may here become limited by carbon assimilation when carbon storage is low. Strictly speaking, growth in THORP-G is more sink-limited than growth in the original THORP, though both versions consider some combination of source- and sinklimitations. We reduce turgor-driven growth rates in THORP-G when immobile NSC storage is low (Schiestl-Aalto et al. 2019), and growth rates are modified by a Michaelis-Menten function of NSC storage similar to Jones et al. (2019). Additionally, online simulations consider the temperature-dependence of extensibility, which have recently been incorporated in TDGMs (Cabon, Peters, et al. 2020, Peters et al. 2021). We apply the same temperature-dependence as Potkay et al.'s (2021) simulations, which is based on Schiestl-Aalto et al.'s (2015) empirical formulation for Scots Pine. From turgor dynamics alone, it is reasonable to hypothesize that most growth occurs during nighttime or early morning when water potentials are least-negative (Steppe et al. 2015). Indeed, Zweifel et al. (2021) have recently demonstrated that mature trees in Swiss forests grow predominantly at night. However, if osmotic regulation strengthens osmotic potentials enough to compensate for daytime water potentials, then the difference between daytime and nighttime growth rates may be small under well-watered conditions (compare purple lines in Figure 1g and h). The additional effects considered here from NSC and temperature on growth in THORP-G further modulate when the most and least

Table 2. Key parameters in THORP-G simulations and their literature source. One THORP parameter,  $r_{SW}^{n}_{15}$ , was changed for THORP-G simulations

Symbol	Meaning	New value	Old value	Units	Source
φ	Extensibility	2.3•10 <sup>-7</sup>	_	MPa <sup>-1</sup> •s <sup>-1</sup>	Steppe et al. (2006, 2008), Salomón et al. (2019), Peters et al. (2021)
Γ	Turgor threshold for growth	0.75	_	MPa	Offline analyses from this study; chosen so maximum predicted height would equal the upper limit of observed heights for Scots Pine, 45 m (Figure 2d), and chosen for $^{3}/_{4}$ average metabolic scaling (Figure 2b)
а	Scaling exponent relating distance and stem diameter	1.5	_	_	Niklas and Spatz (2004)
b	Scaling exponent relating stem diameter and phloem thickness	<sup>2</sup> / <sub>3</sub>	_	_	Rosell (2016), Rosell et al. (2017)
$ ho_{cL}$	Leaf carbon density	2•10 <sup>4</sup>	_	(mol C)•m <sup>-3</sup>	Mean of conifer leaf densities from Niinemets (1999) and converted assuming leaves are 50% C by mass
СММ	Michaelis-Menten coefficient for phloem loading	300	_	(mol suc)•m <sup>-3</sup>	De Schepper and Steppe (2010)
<i>r<sub>sW</sub></i> <sup>m</sup> 15	Carbon pool-specific sapwood maintenance respiration rate at 15°C	6.6•10 <sup>-11</sup>	2.2•10 <sup>-12</sup>	s <sup>-1</sup>	Schiestl-Aalto et al. (2015) for Scots Pine

growth occurs diurnally. Hence, THORP-G may capture a variety of diurnal growth responses, including when maximum and minimum growth rates occur (Mencuccini et al. 2017).

We parameterized THORP-G with values reported or estimated from existing literature (Table 2). We note that no parameters were finely tuned to match observations, and by using parameters that are as physically based as possible, we focus on the model's ability to capture fundamental processes. Additional simulations were performed with additional water-stress (reduced precipitation and higher vapor pressure deficit) to explore the hydraulic controls of tree height (Givnish et al. 2014, Tao et al. 2016) or with different values of the turgor threshold,  $\Gamma$ . Predictions are compared with height-age trends (site indices) of the dominant Scots Pine trees in forest stands of Northern Spain (Bravo and Montero 2001, Palahi et al. 2004), where Potkay et al.'s (2021) original THORP simulations were based (Tillar Valley; Poblet Forest Natural Reserve; Prades Mountains). Because site indices generally apply to adequately stocked, even-aged stands, site indices are consistent with THORP's existing structure and thus are well-suited for testing our predictions.

#### **Results**

## Systematic permutation of PTM

Regardless of parameterization (Table 1), predictions of  $\Phi(\tilde{z}=1)^{1/2}$  were concentrated near 1, where  $\Phi(\tilde{z}=1)^{1/2}$  is equal

to the ratio of the sugar concentrations at the root collar and stem apex (Figure 2). Values less than one reflect greater sugar concentrations at the apex than at the root collar. Values greater than one are possible though rare and reflect smaller sugar concentrations at the apex than at the root collar, which becomes more likely to occur as unloading rates in the stem increases relative to the local loading from recently assimilated photosynthates and past storage. Values less than zero do not suggest upward sugar flux at the root collar, since a downward flux is set as boundary condition to satisfy root growth and respiration (see Eq. S.1.21 available as Supplementary data at Tree Physiology Online). Instead, it merely suggests a nonmonotonic sugar concentration profile. A value of one represents no difference across the stem and uniform osmotic potentials. Ninety percent of predictions had  $\Phi(\tilde{z}=1)^{1/2} > \sim 0.9$ , and 80% predicted  $\Phi(\tilde{z}=1)^{1/2} > \sim 0.97$ , suggesting nearly uniform sugar concentrations for a 4.4-m-tall conifer. Similar results were found for a larger, 44-m-tall conifer; however, the distribution of predictions was broader (see Figure S5 available as Supplementary data at Tree Physiology Online; 70 and 80% predictions had  $\Phi(\tilde{z}=1)^{1/2}$  greater than  $\sim$ 0.9 and  $\sim$ 0.8, respectively), suggesting that the sugar dynamics of larger trees are more sensitive to sink demands and conductances than are smaller trees. Nonetheless, most predictions were concentrated at one, suggesting uniformity of phloem sugar concentrations and that uniform osmotic potentials is at least a reasonable firstorder approximation for tall trees. These results contradict our

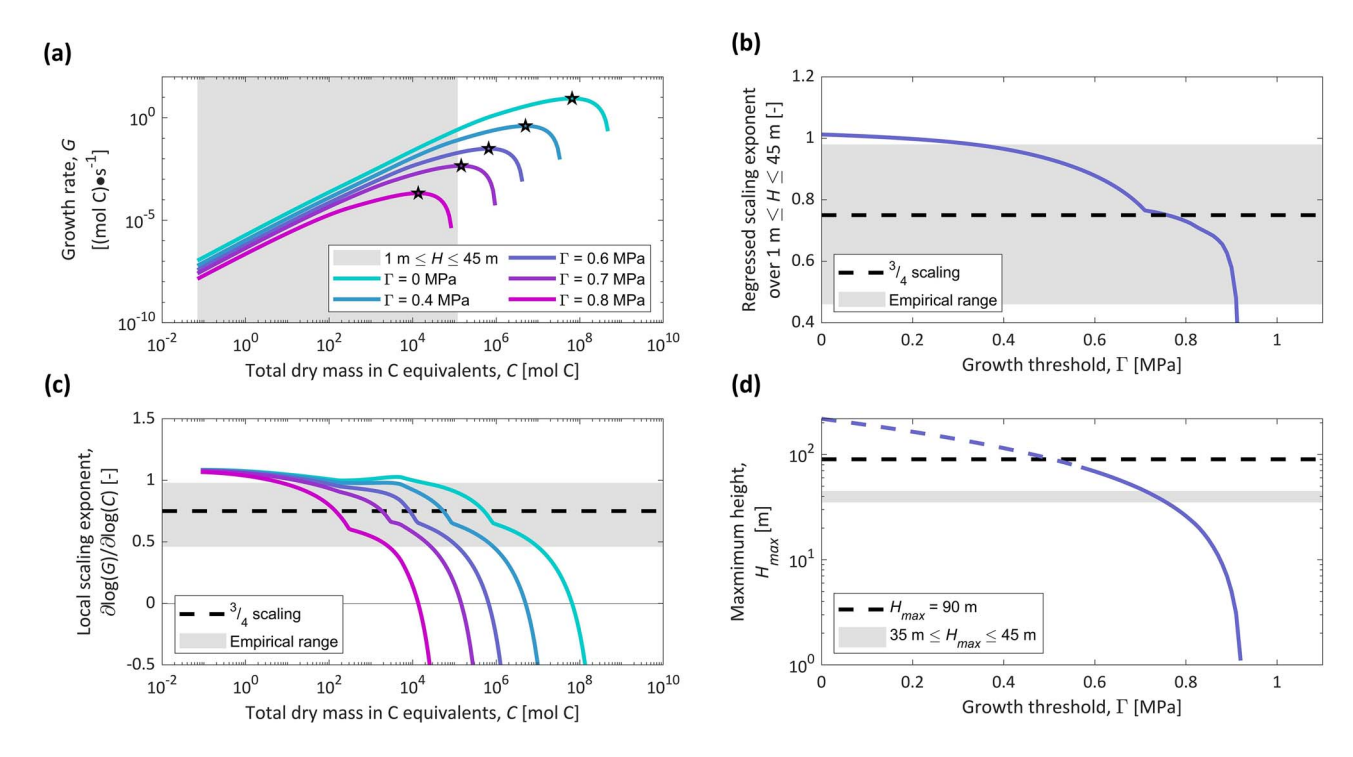


Figure 3. Predictions from offline TDGM simulations, applying predawn leaf water potentials (see Figure S3a available as Supplementary data at *Tree Physiology* Online). (a) Growth rate, G, versus total biomass in carbon equivalents, C, for varied turgor thresholds,  $\Gamma$ . Gray area represents the biomass range for which tree height, H, is between 1 and 45 m, the larger chosen as the upper height limit for most conifers (Tao et al. 2016). Stars represent optimum growth rates. (b) Mean scaling exponent in power-law relating G to C predicted by log-transformed, simple linear regression over the lesser of two biomass ranges: that coinciding with  $1 \le H \le 45$  m (gray area in a) or that coinciding with optimum growth rate (stars in a). (c) Local, tree size-specific scaling exponent,  $\partial \log(G)/\partial \log(C)$ . Dashed, black lines in (b) and (c) denote the idealized  $^3/_4$  scaling. Gray areas in (b) and (c) represent the empirical range in scaling exponents (Coomes and Allen 2009, Muller-Landau et al. 2006, Smith and Sperry 2014). (d) Maximum height,  $H_{\text{max}}$ , estimated as height coinciding with optimum growth rate (stars in a), versus turgor threshold,  $\Gamma$ . Solid, blue line is the predicted  $H_{\text{max}}$  that coincides with the range of water potentials measured by Paljakka et al. (2017) on scots pine, whose regression we used to predict osmotic potentials. Dashed, blue line is the  $H_{\text{max}}$  predicted by extrapolating Paljakka et al.'s (2017) regression. Dashed, black line denotes a height of 90 m, the upper height of Giant sequoia conifers. Gray area represents the range of observed maximum heights of scots pine.

first hypothesis that axial phloem transport must be considered explicitly to accurately predict turgor distributions and thus turgor-driven growth, greatly simplifying the TDGM and allowing us to approximate the entirety of the stem osmotic profile by the apex osmotic potential.

#### Offline simulations of TDGM

For realistic turgor thresholds (0  $\leq \Gamma \leq$  1 MPa), tree growth rates scaled isometrically (meaning  $\beta=1$ ) at small sizes, regardless of the value for  $\Gamma$  (Figure 3a and c).  $\beta$  generally agreed with empirical estimates for a broad range of  $\Gamma$  ( $\sim$ 0.3 <  $\Gamma$  <  $\sim$ 0.9 MPa) when either interpreted by log-transformed, simple linear regression over realistic biomass ranges (Figure 3b) or calculated locally (i.e.,  $\partial \log(G)/\partial \log(C)$ ; Figure 3c), supporting our second hypothesis that sink-limited growth is consistent with observed and theorized metabolic scaling. Metabolic scaling became less isometric in larger trees ( $\beta$  < 1; Figure 3a and c), as water potentials became more negative (see Figure S4 available as Supplementary data at Tree Physiology Online), further supporting our second hypothesis' corollary that size-mediated changes in turgor shape  $\beta$ .

Growth behaved non-monotonically with biomass, reaching an optimum depending on  $\Gamma$  (stars in Figure 3a), leading us to perform a post hoc analysis of maximum tree heights,  $H_{max}$ . We expect that these optima coincide with  $H_{\text{max}}$  for one of two possible reasons, and thus, the model may explain observed  $H_{\text{max}}$ . The first reason is that trees may have evolved their  $H_{\text{max}}$ to optimize growth and compete with neighbors (King 1990, Mäkelä 1985), and once reaching the optimum height, height increases stop and excess axial woody biomass is redirected radially (Kira 1978). The second reason is that growth rates drop by orders of magnitude soon after their optimum due to increasingly negative water potentials (Figure 3a), and thus, trees may grow slightly taller than  $H_{\text{max}}$ ; however, little further progress would be made if maintaining the same trajectory, in which case these optima coincide with approximate estimates for  $H_{\text{max}}$ . The TDGM's predictions of  $H_{\text{max}}$  decline with increasing  $\Gamma$  (Figure 3d). The certainty of these predictions is limited to  $\Gamma > \sim 0.5$  MPa ( $H_{\rm max} \leq \sim 90$  m) by the scope of the empirical regression applied to predict osmotic potentials from  $\psi_S$  (Paljakka et al. 2017). Salmon et al. (2020) measured water and osmotic potentials on Scots Pine and found similar statistical relationships as Paljakka et al. (2017); however, for shorter pines under more-negative water potentials (see Figure S1 available as Supplementary data at *Tree Physiology* Online). The similarity suggests that it may not be totally unreasonable to extrapolate Paljakka et al.'s (2017) regression to more-negative  $\psi_S$ . Upon extrapolation,  $H_{\text{max}}$  increases to  $\sim$ 220 m at negligible  $\Gamma$ . Similar results for metabolic scaling and maximum height were found when considering midday water potentials (see Figures S6 and S7 available as Supplementary data at *Tree Physiology* Online).

These considerations for  $H_{\text{max}}$  are conceptually linked to our third hypothesis that turgor-driven growth can predict height trends. In light of these results, we performed additional offline simulations to demonstrate the sensitivity of the TDGM's predictions of  $H_{\text{max}}$  to water availability. In these additional offline simulations, we apply predawn water potentials given by Potkay et al.'s (2021) past simulations of Scots Pine growth under various precipitation levels (100, 75 and 50% of control). We compare TDGM predictions at multiple values of  $\Gamma$  to Tao et al.'s (2016) global data set of observed maximum tree heights. We recognize that this comparison is imperfect, since our TDGM predictions represent the variability of single species within a site exposed to different hydrologic conditions, while Tao et al.'s (2016) reflects variability among sites and species. Nonetheless, this comparison provides a first-order evaluation. Regardless of  $\Gamma$ , maximum heights decline with precipitation (Figure 4). At full precipitation, TDGM predictions agree best with observations when  $\Gamma$  is large ( $\Gamma > \sim 0.7$  MPa). In contrast, TDGM predictions with small  $\Gamma$  ( $\Gamma$  <  $\sim$ 0.5 MPa) match observations under reduced precipitation. However, large  $\Gamma$  under-predicted heights at low precipitation, and small  $\Gamma$ over-predicted heights at high precipitation (Figure 4).

#### Online simulations of TDGM

Online simulations of height growth rates fall well within observed ranges from nearby stands (Figure 5), supporting our third hypothesis that TDGMs can predict growth rates and height-age relations. While our offline predictions predict  $H_{\text{max}}$ , they cannot say for how long or at what age any height is reached. Our online simulations introduced this additional dimension, explicitly solving for changes in height over time. Both reduced precipitation and higher vapor pressure deficit (through reduced atmospheric relative humidity) increased water-stress, caused more negative water potentials (through explicit calculation of xylem hydraulics and stomatal regulation in THORP) and slowed height growth and produced more curvilinear trends, further slowing growth with age (Figure 5). Larger  $\Gamma$  relative to the control slowed growth and produced more linear behavior, while smaller  $\Gamma$  accelerated growth, produced more curvilinear trends and often caused sink-demand to exceed source availability, leading to premature carbon depletion (Figure 6).

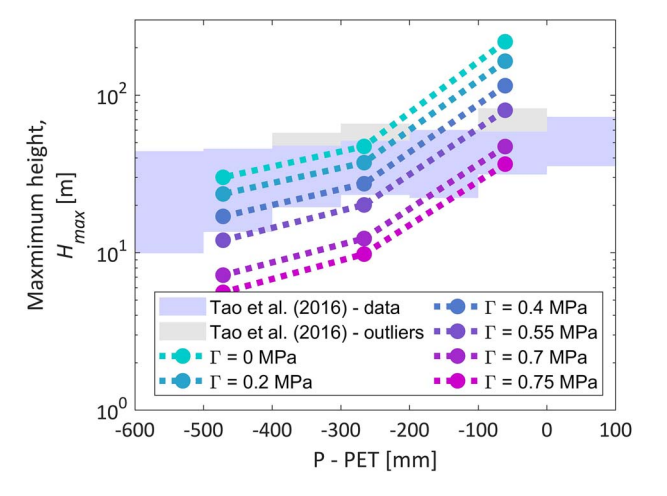


Figure 4. Maximum tree height predicted from offline TDGM simulations applying water potentials under diminishing precipitation from Potkay et al. (2021) (100, 75 and 50% of their control simulation) for multiple values of the turgor threshold for growth,  $\Gamma$ . Predictions are plotted in terms of annual precipitation, P, minus annual potential evapotranspiration, PET, to compare with Tao et al.'s (2016) global data set of maximum tree heights at 1 mm increments of P–PET. Both P and PET were calculated from Potkay et al.'s (2021) atmospheric forcing conditions, and PET was calculated particularly according to the Thornthwaite equation like Tao et al. (2016). We plot the range of maximum heights (shaded areas) reported by Tao et al. (2016) at 100-mm intervals of P–PET due to the limited resolution of their plots from which we extracted their data. We distinguish outliers (light gray shaded area) from the rest of Tao et al.'s (2016) data (light purple shaded area).

Potkay et al.'s (2021) source-limited growth scheme grew faster than both the control, sink-limited scheme ( $\Gamma = 0.75$  MPa) and observations (Figure 6). Compared with the control sink-limited scheme ( $\Gamma = 0.75$  MPa), the source-limited scheme grew  $\sim 1.4$  times faster on average when calculated over the 10 year periodicity of THORP's recycled atmospheric forcing (see Figures 6 and S8a available as Supplementary data at Tree Physiology Online). The sourcelimited scheme grew ~2 times faster at the beginning of the simulation, and the source-sink growth ratio then gradually declined, reaching approximately equivalent growth rates a century later (see Figure S8a available as Supplementary data at Tree Physiology Online). Over annual timescales, however, the height growth ratio between the two schemes varied between  $\sim$ 0.5 and  $\sim$ 6 depending on the year and the degree of sinklimitation (see Figure S8a available as Supplementary data at Tree Physiology Online). The greater variability in the growth ratio at shorter timescales suggests that the source-limited scheme grew fastest relative to the sink-limited scheme when trees from both schemes grew little, further suggesting that sinklimited growth is more sensitive to stress than source-limited growth. While the source-limited scheme always grew at least as fast as the sink-limited scheme if not faster, source-limited growth rates were more sensitive to tree-size, leading to larger

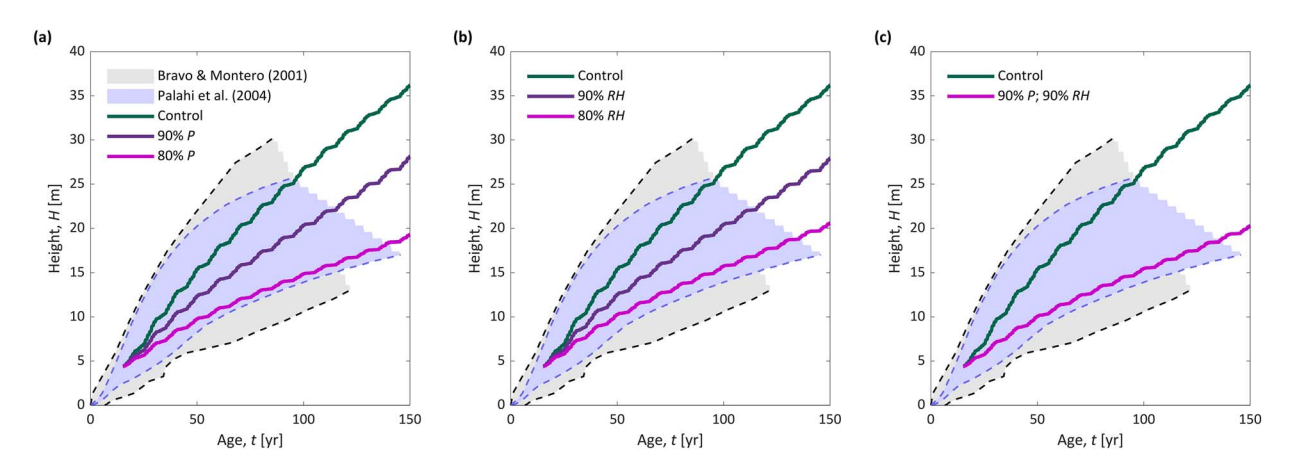


Figure 5. Online TDGM predictions of tree height versus age. Simulations performed with varying precipitation, *P* (a), atmospheric relative humidity, *RH* (b), and precipitation and relative humidity (c). Gray area shows bounds of height-age observations (site indices) for scots pine broadly from NE Spain (Bravo and Montero 2001). Blue area shows height-age observations for scots pine from three provinces in NE Spain (Palahi et al. 2004) that either are near (Huesca and Lérida provinces) or contain (Tarragona province) the site where simulations are based (Potkay et al. 2021). We assume that the initially 4.4-m-tall scots pine is 15 years old.

declines in growth rates at larger sizes (see Figure S8b and c available as Supplementary data at *Tree Physiology* Online) and more asymptotic growth (Figure 6) than in the sink-limited scheme. The variability in growth ratio between the schemes over annual timescales peaked at the middle of the simulation when trees were medium-sized (see Figure S8a available as Supplementary data at *Tree Physiology* Online), coinciding with high variability in source-limited growth (see Figure S8b available as Supplementary data at *Tree Physiology* Online). Source-limited growth of taller trees was less variable (see Figure S8b available as Supplementary data at *Tree Physiology* Online), and the variability of sink-limited growth rates changed little with tree-size (see Figure S8c available as Supplementary data at *Tree Physiology* Online).

Daily growth rates varied by orders of magnitude within a size class (Figure 7a-c), corresponding to daily variations in water potentials and temperature. The upper envelope of daily growth rates, however, followed isometric scaling ( $\beta = 1$ ) as expected from the form of Eq. 3 (Figure 7a-c). When growth was integrated over annual timescales, more allometric behavior  $(\beta < 1)$  can be seen as annual G approximately follows a <sup>3</sup>/<sub>4</sub> power-law scaling on average (Figure 7d–f), further supporting our second hypothesis that sink-limited growth is consistent with observed and theorized metabolic scaling. Confidence intervals for annual G at a given C expanded at larger sizes, and the upper and lower envelopes were bound by isometric and  $^{1}/_{2}$  power-law scaling curves ( $\beta = ^{1}/_{2}$ ) (Figure 7d–f), agreeing with empirical ranges for  $\beta$  (0.46–0.98; Muller-Landau et al. 2006; Coomes and Allen 2009; Smith and Sperry 2014). These exponents correlated with water availability, such as annual precipitation (see Figure S9a and b available as Supplementary data at Tree Physiology Online), with larger exponents in wetter years, consistent with notions that resource limitations effect scaling (Coomes and Allen 2009, Muller-Landau et al. 2006). Exceptionally, wet years sometimes followed dry years or vice versa, partially obscuring the relationship between annual precipitation and  $\beta$  (see Figure S9a and b available as Supplementary data at *Tree Physiology* Online). The relationship between water availability and  $\beta$  became clearer when considered in terms of annually averaged soil moisture (see Figure S9c and d available as Supplementary data at *Tree Physiology* Online), especially after detrending for tree-size effects on soil water availability (see Figure S9e and f available as Supplementary data at *Tree Physiology* Online). These results further support our second hypothesis, particularly its corollary that water-stress induced changes in turgor shape  $\beta$ .

## **Discussion**

Axially uniform phloem sugar concentrations and osmotic potentials

Our PTM (Eq. 1) and permutation analyses suggest that phloem sugar concentrations and osmotic potentials are nearly axially uniform along tree stems in steady-state and when sink-limited, contrary to our first hypothesis that phloem transport must be considered explicitly to accurately predict turgor distributions and thus turgor-driven growth. We provide strong theoretical evidence for osmotic uniformity in small trees (Figure 2) that may weaken in larger trees but still offers a reasonable first-order approximation (see Figure S5 available as Supplementary data at *Tree Physiology* Online). These results do not suggest, however, that sugar concentrations are constant, since studies provide ample evidence that osmolyte concentrations vary diurnally (Chan et al. 2016, Lazzarin et al. 2019). Instead, we suggest that sugar concentrations should vary little spatially between stem apex and root collar in steady-state. Though

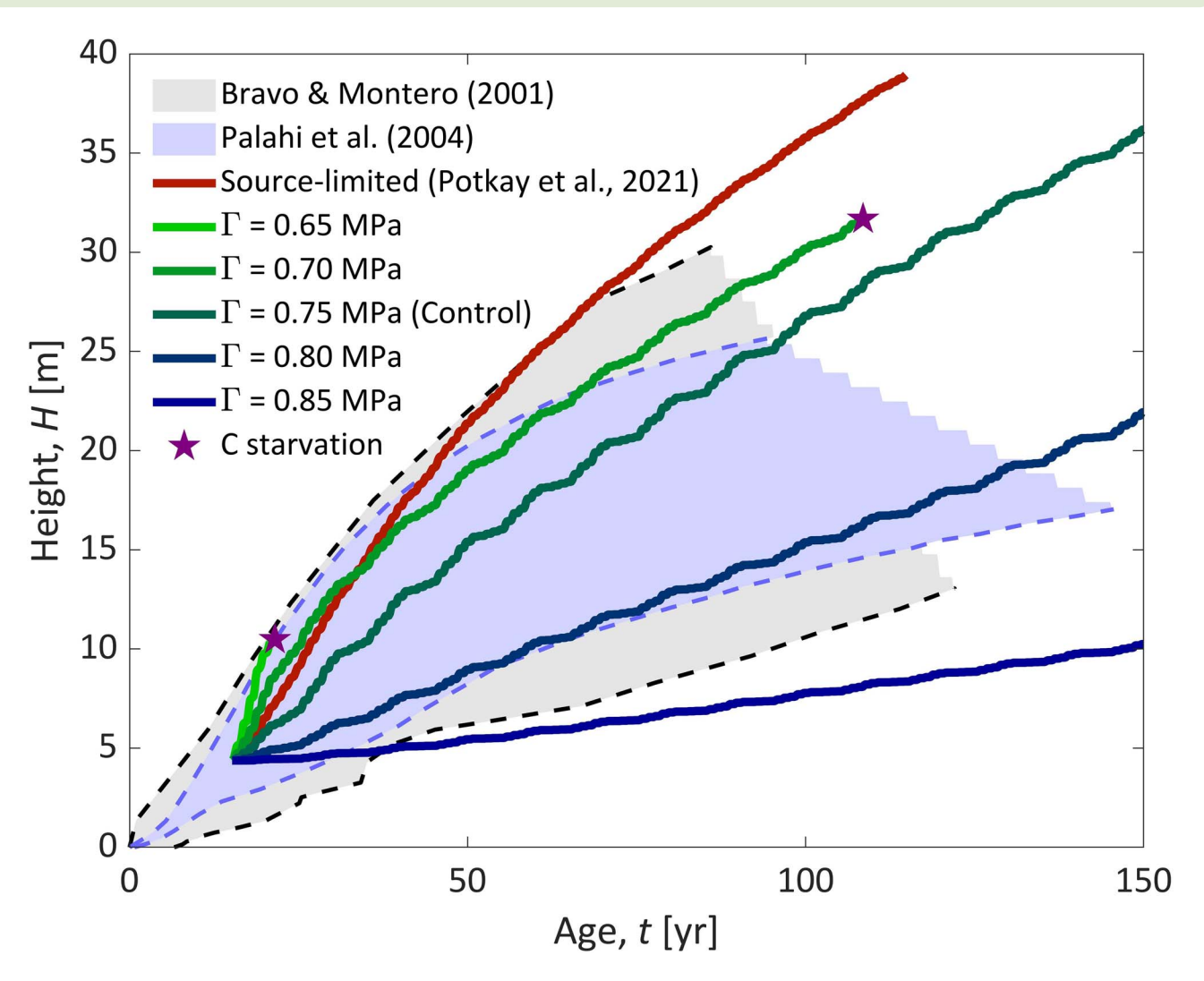


Figure 6. Online TDGM predictions of tree height versus age. Simulations performed with varying turgor threshold for growth,  $\Gamma$ , and Potkay et al.'s (2021) source-limited simulation. Purple stars denote mortality events by carbon starvation, here defined as insufficient carbon storage for osmoregulation. Blue area shows height-age observations for scots pine from three provinces in NE Spain (Palahi et al. 2004) that either are near (Huesca and Lérida provinces) or contain (Tarragona province) the site where simulations are based (Potkay et al. 2021). We assume that the initially 4.4-m-tall scots pine is 15 years old.

our results do not support our first hypothesis, they support alternative hypotheses such as the osmoregulatory flow (Thompson and Holbrook 2003b, 2004) and high pressure manifold (Patrick 2013) hypotheses. According to the osmoregulatory flow hypothesis, turgor pressure differentials should be small or negligible. Such a system would be extremely convenient to control, since all organs irrespective of their location would receive the same stimulus (Thompson and Holbrook 2003b) and would efficiently propagate pressure waves (Thompson and Holbrook 2004), which are theorized to quickly relay information throughout plants. Similarly, the high pressure manifold hypothesis states that phloem transport is limited by unloading at sinks rather than by axial hydraulic resistances, leading to a system in which solute concentrations are high and axial pressure differentials in the phloem are small. These hypotheses have found empirical support in trees (Patrick

2013 and references therein; Paljakka et al. 2017; Savage et al. 2017; Lazzarin et al. 2019), and near uniform turgor is simulated by similar PTMs with spatially distributed sinks (De Schepper and Steppe 2010).

Other PTMs lack distributed carbon sink along stems and do not often simulate uniform turgor (Hölttä et al. 2006, 2009, Jensen et al. 2012, Thompson and Holbrook 2003a). These PTMs, however, can predict increasingly uniform turgor profiles as phloem become more conductive relative to xylem (Hölttä et al. 2009). Some studies report decreasing ratios of phloem to xylem conductivity with tree-size (Hölttä et al. 2013, Jyske and Hölttä 2015), suggesting less uniform turgor in taller trees and similar to our results (Figures 2 and S5 available as Supplementary data at *Tree Physiology* Online). It is noteworthy that these studies calculated conductivities from sieve element number and conduit radii according to the Hagen–Poiseuille

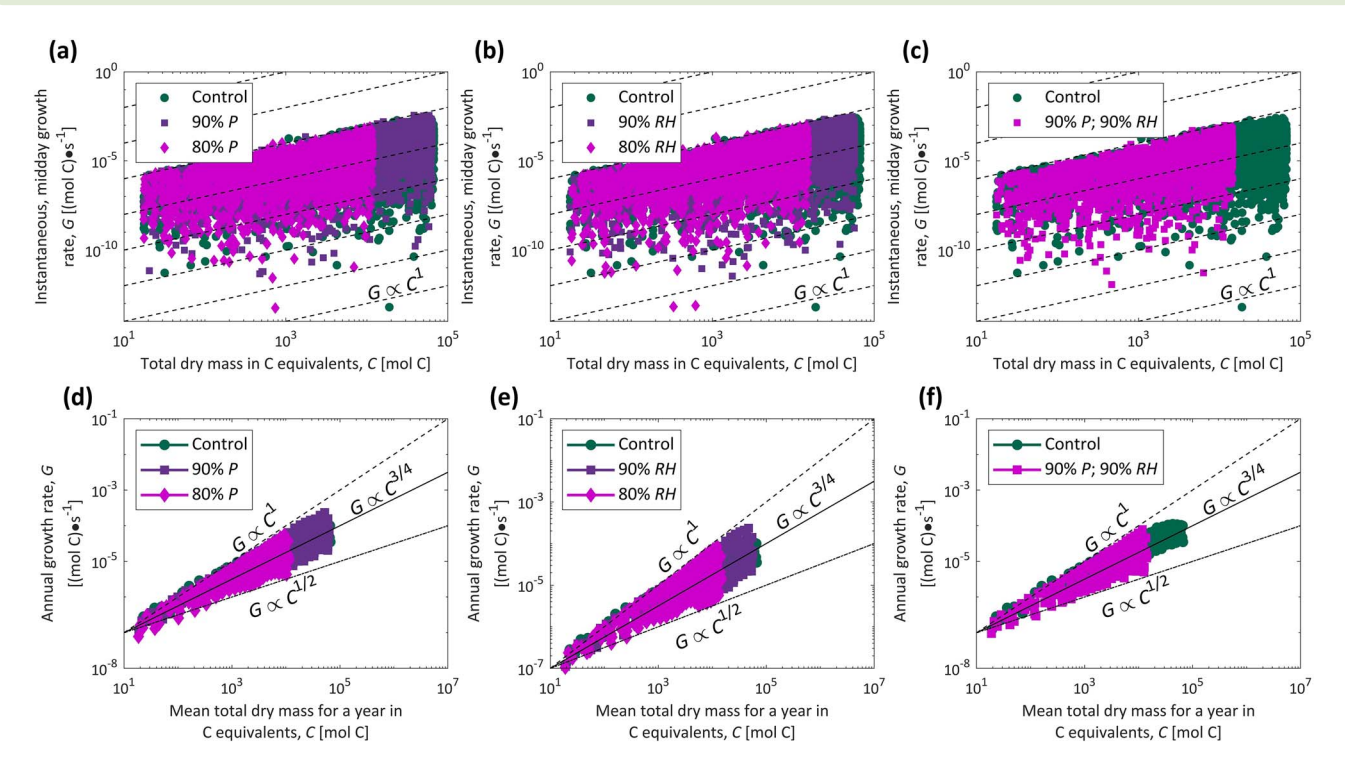


Figure 7. Predictions from online TDGM simulations of scaling of instantaneous (a—c) and annual-integrated (d—f) growth rates, G, versus total biomass in carbon equivalents, C. Simulations performed with varying precipitation, P (a,d), atmospheric relative humidity, RH (b,e), and precipitation and relative humidity (c, f).

equation, assuming sieve end-wall resistances are proportional to conduit resistances by a fixed fraction independent of size. Recently, several studies have investigated these sieve endwall resistances and how they scale with stem size (Clerx et al. 2020, Liesche et al. 2017, Losada and Holbrook 2019, Savage et al. 2017), the consideration for which may potentially alter how the ratio of phloem to xylem conductivity scales with tree-size. Nonetheless, the scaling of phloem and xylem conductivities plays an important role in phloem's turgor profile. Our PTM predicts nearly uniform osmotic potentials regardless of how exactly phloem conductance scales within a tree or with size. Uniform osmotic profiles are maintained by conductances that are large enough to support the proportionally small sinkdemands (i.e., growth and respiration rates), suggesting that phloem transport itself is sink-limited and responds directly to sink demands (Lemoine et al. 2013). This notion is consistent with abundant evidence supporting that phloem conductance does not generally exert any control on sink growth (Gifford and Evans 1981) and further suggests a redundancy of phloem transport in the stem similar to the redundancy of stem xylem transport (Dietrich et al. 2018). This osmotic uniformity does not result solely from the magnitude of sink demands but results also from the realistic distribution of carbon sinks along stems and belowground. Indeed, when a carbon sink is added along the stem and then incrementally strengthened, other PTMs simulate increasingly uniform osmotic potentials (Seleznyova and Hanan 2018).

In light of these findings, observations of slowed phloem transport under drought (Dannoura et al. 2019, Ruehr et al. 2009) may result from reduced sink demand rather than reduced phloem transport capacity. Under drought, phloem conductance declines due to increased sugar concentrations and viscosity and smaller sieve tube (Dannoura et al. 2019, Woodruff 2014); however, this decline is not large enough to challenge transport, often leading to the interpretation of a reduced turgor gradient (Dannoura et al. 2019, Sevanto 2014). We show that this large turgor gradients are not necessary to support sink activity, and drought-induced slowed transport may be alternatively explained by reduced sink demand. Under drought, water potentials become more negative, and turgor decreases, thereby reducing sink demand by slowing cell expansion (Lockhart 1965), division (Kirkham et al. 1972) and potentially maintenance respiration (Saveyn et al. 2007), and slowing phloem transport as well. Our results (Figures 2 and S5 available as Supplementary data at *Tree Physiology* Online) consider the phloem transport within stems explicitly and the remaining organs only implicitly. Thus in addition to reduced demand and unloading, phloem transport may be limited under extreme drought by reduced transport capacities elsewhere (e.g., conductances and loading in leaves) or by biotic stresses such as attacks by pathogens and herbivores (Salmon et al. 2019).

## Turgor-limited metabolic scaling

Offline simulations of our TDGM predicted realistic  $\beta$  with behavior depending on thresholds,  $\Gamma$  (Figure 3b), supporting our second hypothesis that growth-scaling of trees can be explained by turgor-driven growth. Online simulations with THORP-G corroborated these offline predictions (Figure 7). Metabolic scaling is observed over many orders of magnitude of whole-tree biomass ( $\sim 10^{-3}$  to  $\sim 10^4$  kg dry matter; Cannell 1982), the timescales of which span decades to centuries and the lifespan of a tree. Hence, these results support the application of TDGMs over these timescales, which are far longer than the past, several yearlong experiments in which TDGMs have been validated (Cabon, Fernández-de-Uña, et al. 2020, Cabon, Peters, et al. 2020; Coussement et al. 2020). In addition to supporting TDGM application for prediction, these results further suggest that turgor is a fundamental limitation in tree growth.

Regardless of  $\Gamma$ ,  $\beta$  decreased as trees grew larger (Figure 3b), consistent with observations that growth of larger trees follows smaller exponents (Muller-Landau et al. 2006) and may even progressively decline radially past a critical size (Fritts 1976; Figure 3a). The reduction in scaling was produced here from hydraulic limitations (Ryan and Yoder 1997), particularly the longer hydraulic paths and larger xylem resistances in taller trees, resulting in more-negative water potentials (see Figure S4 available as Supplementary data at Tree Physiology Online; Koch et al. 2004). These water potentials translate to growth through turgor, which limits both vertical (Marshall and Monserud 2003, Woodruff et al. 2004, Woodruff and Meinzer 2011) and radial growth (Cabon, Fernández-de-Uña, et al. 2020, Cabon, Peters, et al. 2020, Peters et al. 2021). Morenegative water potentials in larger trees reduce their turgor, slow their growth and here alter their growth scaling in line with our second hypothesis' corollary that size-mediated turgor changes shape  $\beta$ . Similarly, others have demonstrated that metabolic scaling exponents decline with plant size (Mori et al. 2010, Reich et al. 2006); however in these studies, metabolic rate was measured via respiration, not growth. Nonetheless, our TDGM's underlying mechanism of size-mediated turgor declines may explain this respiratory scaling, since turgor and its corollary, tissue water content, limit maintenance respiration (Huang et al. 2020, Saveyn et al. 2007). Indeed, size-mediated reductions in water content are known to reduce the metabolic scaling of respiration (Huang et al. 2020, Peng et al. 2010).

In addition to our TDGM's ability to capture size-mediated reductions in  $\beta$ , it also captures other empirical behaviors in which other theories have difficulty in explaining (Enquist and Niklas 2002, West et al. 1999). Our online simulations demonstrate that turgor's control on metabolic scaling does not emerge solely from size-mediated changes in internal hydraulics

but also arises from external water availability, predicting smaller exponents during drier periods (see Figure S9 available as Supplementary data at Tree Physiology Online), supporting our second hypothesis' corollary that water-stress induced turgor changes shape  $\beta$ . Past literature has shown that resource limitations reduce  $\beta$  (Coomes and Allen 2009, Muller-Landau et al. 2006); however, these limitations to growth are often discussed in terms of light, but rarely water. Nonetheless, stands with less precipitation tend to have lower  $\beta$  (Muller-Landau et al. 2006). Support for the hypothesis that light availability shapes  $\beta$  may truly reflect size-dependent behavior, as discussed in the previous paragraph. Light access is related to tree-size (Sheil et al. 2006), and several studies demonstrated that tree-size affects  $\beta$  to imply that light access controls  $\beta$  but did not strictly uncouple light- and size-effects (Coomes and Allen 2009, Russo et al. 2007). When the effects of light and size are considered separately, they predict growth equally well (Wyckoff and Clark 2005). Interestingly, our TDGM also predicts larger  $\beta$  for trees with taller maximum heights and larger growth rates (Figure 3), consistent with observations (Coomes et al. 2011, Li et al. 2005, Russo et al. 2007), and which have been explained previously also in terms of light access. Our TDGM equally explains these scaling behaviors qualitatively through turgor. Light must play some role; however, differences between light and turgor are analogous to differences between source- and sink-limitations, respectively (Fatichi et al. 2014). As growing evidence supports generally sink-limited plant growth (Körner 2015, Millard et al. 2007), a sink-limited perspective for metabolic scaling must also be duly considered.

## Tree height and hydraulic limitations

Turgor-limitations have been long hypothesized as the control on height and canopy growth (Waring and Schlesinger 1985), which are increasingly tested and find support (Woodruff et al. 2004, Woodruff and Meinzer 2011). The turgor-limitation hypothesis may be considered a sink-limited modification of the hydraulic limitation hypothesis (Ryan et al. 2006, Ryan and Yoder 1997). Both the turgor-limitation and hydraulic limitation hypotheses pose that height is limited by trees' ability to conduct water, reducing water potentials (Koch et al. 2004) and exacerbated by taller trees' higher vulnerability to embolism (Olson et al. 2018). The classic interpretation of the hydraulic limitation hypothesis is that the more-negative water potentials in taller trees induce stomatal closure, reduce photosynthetic carbon assimilation and thus generate a source-limitation to height. While taller trees are observed to close their stomata and assimilate less, the reduction in assimilation is too small to challenge growth (Ryan et al. 2006). Alternatively, the turgorlimitation hypothesis states that trees' heights are limited by their water potentials, which reduce turgor and limit tissue expansion as they grow taller. Our TDGM predicts realistic height-age relationships and maximum heights (Figures 3-5)

and reductions in drier environments (Figures 4 and 5), consistent with observations (Givnish et al. 2014, Tao et al. 2016), supporting our third hypothesis that turgor-driven growth explains growth rates and height-age trends. Like our considerations of metabolic scaling, these results further support the application of TDGMs for prediction over decadal to centurial timescales and tree lifespans, and suggest that turgor is a fundamental limitation for tree growth.

Other mechanistic models generally predict tree height from various source-limited concepts, including optimizing light interception (Buckley and Roberts 2006, King 1990, Mäkelä 1985) and such that allometry is constrained by available precipitation and metabolic requirements (Kempes et al., 2011). Recent mechanistic growth models have introduced sink-limitations to study source-sink dynamics, predicting height from both source- and sink-limitations (Hayat et al. 2017, Schiestl-Aalto et al. 2015). These other sink-limited models, however, do not consider turgor, an established physiological control on cell expansion and division (Kirkham et al. 1972, Lockhart 1965). Instead, they model growth directly from the NSC storage size and water-stress empirically (Schiestl-Aalto et al. 2015) or through formulations designed to produce desired behaviors without consideration of their underlying physiological mechanisms (Hayat et al. 2017). To our knowledge, no other model predicts tree height explicitly from turgor and the turgor-limitation hypothesis like ours.

Potkay et al.'s (2021) source-limited growth scheme for THORP grew faster than both THORP-G's sink-limited scheme  $(\Gamma = 0.75 \text{ MPa})$  and observation (Figure 6), supporting the notion that plant growth is generally sink-limited (Körner 2015, Millard et al. 2007). THORP includes a simple representation of growth, in which growth rates are proportional to the size of a single NSC storage size (Potkay et al. 2021). This representation reduces to a source-limited perspective of growth when considered in steady-state. It is unlikely that the excessively fast growth from THORP can be explained by unrealistically large carbon assimilation rates, since Potkay et al. (2021) simulated realistic leaf areas and reasonable, if not slightly small, midday leaf area-specific carbon assimilation rates averaged over the simulation (2.5 ( $\mu$ mol CO<sub>2</sub>) $\bullet$ s<sup>-1</sup> $\bullet$ m<sup>-2</sup>). Thus, THORP's unrealistically fast growth is better explained by its lack of sink-limitation mechanisms to constrain realized growth, which improved growth predictions in the turgor-driven THORP-G. Additionally, Potkay et al. (2021) defined mortality when carbon storage reached zero, while we defined mortality here as insufficient storage for osmotic regulation, which occurs before complete depletion. Potkay et al.'s (2021) source-limited scheme grew faster than sink-limited scheme with  $\Gamma=0.70$  MPa, which failed to osmotically regulate, suggesting source-limited trees would have also failed to osmotically regulate, further indicating the deficiency in assuming solely source-limitations, particularly the assumption that growth is proportional to

photosynthetic carbon assimilation (Enquist et al. 1999, Fatichi et al. 2014).

#### Role of the turgor threshold, $\Gamma$

Both of our offline and online TDGM simulations emphasize the importance of  $\Gamma$ , the threshold in the Lockhart (1965) equation which turgor, P, must exceed before expansion occurs. Offline simulations demonstrate how  $\Gamma$  controls the metabolic scaling exponent,  $\beta$  (Figure 3), and both offline and online simulations show how it controls tree height (Figures 3, 4 and 6). Online simulations with small thresholds ( $\Gamma \leq 0.7$  MPa) overly accelerated growth, causing sink-demand to exceed source availability and leading to premature carbon depletion, defined here as insufficient carbon storage for osmotic regulation (Figure 6). This carbon depletion could have been avoided had we parameterized the online simulations with a smaller extensibility,  $\phi$ . However, significantly smaller  $\phi$  may not be physiologically realistic. The value for  $\phi$  of 2.3ullet10<sup>-7</sup> MPa<sup>-1</sup>ullets in these simulations (Table 2) is from the lower limit of previously reported  $\phi$  estimates from the literature for woody expansion (Cabon, Fernández-de-Uña, et al. 2020). Some literature reports values for trees that span approximately double (Saveyn et al. 2007, Steppe et al. 2008) to one or two orders of magnitudes larger (De Schepper and Steppe 2010). Similarly, alternative yet realistic values of a and b would not significantly reduce G. Hence, carbon depletion in simulations with smaller  $\Gamma$  is likely inevitable even with alternative parameterizations.

Little is known about  $\Gamma$  and what controls it, especially for whole stems which TDGMs represent. Several studies have assumed  $\Gamma = 0.9$  MPa and have accurately simulated changes in stem diameter (Génard et al. 2001, Peters et al. 2021, Steppe et al. 2006, 2008). This commonly applied value for  $\Gamma$  was originally taken as the upper limit of measured values of  $\Gamma$  (0.6– 0.9 MPa; De Schepper and Steppe 2010), assuming that  $\Gamma$ is higher for stem tissues than for young tissues or individual cells (Génard et al. 2001). The assumed  $\Gamma = 0.9$  MPa is rarely questioned, since many TDGMs are relatively insensitive to  $\Gamma$ (e.g., Cabon, Fernández-de-Uña, et al. 2020, De Schepper and Steppe 2010, Steppe et al. 2006). Nonetheless, this value is similar to our estimate of 0.75 MPa, which produced maximum trees height consistent with those for Scots Pine (Figure 3d) and  $^{3}/_{4}$  metabolic scaling (Figure 3b). However,  $\Gamma > \sim 0.85$  MPa in our TDGM results in unrealistic metabolic scaling and heights (Figures 3 and 6), suggesting that the exact value of  $\Gamma$  is consequential and worthy of further consideration. How does  $\Gamma$  vary among environments and species? No studies to our knowledge have attempted to answer this question at the tissue scale, and few studies have investigated the environmental controls on  $\Gamma$  at cellular scales (Frensch and Hsiao 1995, Nakahori et al. 1991, Pritchard et al. 1990).

Comparison of our TDGM to observed tree heights (Figure 4) suggests that trees species adapted to mesic environments have

larger  $\Gamma$  or are less efficient at maintaining P under waterstress than tree species adapted to xeric environments. Such a response in  $\Gamma$  would be analogous to wall stress relaxation and polymer creep in individual cells (Cosgrove 1997), which may maintain nearly constant  $P-\Gamma$  despite changes in P (Green et al., 1971). Conversely, meta-analyses have shown that plants adapted to more xeric environments tend to maintain higher P for a given water potential (Bartlett et al. 2012, Zhu et al. 2018). P and  $\Gamma$  should be tightly coordinated so atypical turgor losses stimulate slowing or shutdown of growth to conserve NSC for maintenance under stress (Körner 2003). According to this interpretation, the  $P-\Gamma$  difference would reflect the plant's caution, where larger  $P-\Gamma$  suggests a risker strategy that maintains higher growth rates during drought though at a higher danger of exhausting NSC and thereby potentially reducing post-drought growth rates. Thus,  $P-\Gamma$  may mediate a tradeoff between during drought and post-drought growth (e.g., Gazol et al. 2017). Hence, we expect that species adapted to wetter conditions have larger  $\Gamma$  at the whole stem scale and operate at higher P under typical conditions, though at higher vulnerability to turgor loss under drought. We recognize, however, that interpreting typical turgor pressures from ecosystem alone may not be simple, since it would be complicated by different species' strategies for stomatal regulation (Fu and Meinzer 2019, Meinzer et al. 2016) and osmotic regulation (Bartlett et al. 2012), which control the two parts of turgor, water potentials and osmotic potentials, respectively.

## Applicability of TDGMs in DGVMs

Applying uniform osmotic potentials simplified the mathematical solution of our TDGM (Eq. 4) and greatly reduced its computation by not having to couple with the PTM. Additionally, by not coupling the PTM, we reduced the number of parameters required for the TDGM (Table 1). The mathematical and parametric simplicity of our TDGM suggests that mechanistic, sink-driven modeling of growth is feasible in DGVMs (Fatichi et al. 2014, 2019, Körner 2015), contrary to past expectations that TDGMs may be too complex for integration into DGVMs (e.g., Babst et al. 2018). Note that we here defined our parameters,  $\phi$ ,  $\alpha$  and b (Eqs 3 and 4), separately according to their physiological meanings (Table 2); however, the three parameters could be lumped together into single parameter (i.e.,  $\phi \bullet (1 + 2a) \bullet (ab)^{-1}$ ) to reduce the total number of parameters, since their combined effects on growth are purely multiplicative (Eqs 3 and 4). Though our approximation of uniform osmotic potentials becomes uncertain for tall trees (see Figure S5 available as Supplementary data at Tree Physiology Online), our TDGM nonetheless predicts realistic growth and compares well to allometric theory, with which few DGVMs agree (Wolf et al. 2011). Turgor-driven, sink-limited mechanisms improved predictions of growth compared with a

source-limited alternative, which grew faster than both observations and our TDGM (Figure 6). In virtually all DGVMs, growth is driven by solely photosynthesis without considering sinklimitations (Fatichi et al. 2014, Friend et al. 2019). Despite improved predictions by considering sink-limitations, few studies have addressed environmental sink-limitations empirically at large-scales (Eckes-Shephard et al. 2021, Guillemot et al. 2017, Leuzinger et al. 2013), and fewer have considered internal limitations (Jones et al. 2019). Our results suggest that sink-limited mechanisms should be better represented in DGVMs to understand and accurately predict the future of the terrestrial carbon cycle. Furthermore, our TDGM captures tree growth's sensitivity to water-stress (Figure 5; Muller et al. 2011; Lempereur et al. 2015), especially for larger trees (see Figure S8b and c available as Supplementary data at Tree Physiology Online), which are theorized to be more sink-limited (Hayat et al. 2017; shown here by declining  $\beta$ ; Figure 3c). Our TDGM's sensitivity suggests that future increases in drought frequency and severity (IPCC 2019) will impair growth, accelerating carbon cycle feedbacks and reducing future carbon sequestration in climate predictions.

Others have recently implemented novel growth schemes in large-scale vegetation models (Eckes-Shephard et al. 2021, Jones et al. 2019, Mina et al. 2016), improving predictions of growth and carbon fluxes compared with traditional and solely source-limited schemes. Jones et al. (2019) focused on NSC availability and limitations to capture NSC storage's potential buffering of growth during periods of little assimilation. They implemented their model, SUGAR, in a land surface model (JUULES) and thereby improved the accuracy of predictions of carbon fluxes during a large-scale Amazon drought experiment. Our simple TDGM takes a very similar mathematical form as SUGAR, in which growth is proportional to biomass and limited by NSC storage (compare our Eg. S.3.4, available as Supplementary data at *Tree Physiology* Online, versus their Eq. 4), further suggesting that simplified TDGMs can be implemented in DGVMs. Improving upon SUGAR, our TDGM also accounts for the physiological and turgor-mediated roles of plant hydraulics, hydraulic limitations and the continual reduction in growth under worsening water-stress (Lempereur et al. 2015). Similar to SUGAR, Mina et al. (2016) and Eckes-Shephard et al. (2021) have recently implemented simple, sink-limited schemes in dynamic vegetation models (ForClim and HYBRID9). Rather than focusing on NSC storage, Mina et al. (2016) and Eckes-Shephard et al. (2021) both accounted for reductions in stem growth due to water limitations. Proceeding from traditional wood formation models (e.g., Fritts et al. 1991, Vaganov et al. 2006), Mina et al. (2016) and Eckes-Shephard et al. (2021) parameterized radial growth as piecewise linear functions of soil moisture and soil water potential, respectively. Their choices of soil moisture and soil water potential are inconsistent with turgor-driven growth, considering stem

growth depends on the turgor and water potential in stems, which become decoupled from soil water potentials under high atmospheric demand (Cabon, Peters, et al. 2020). Stem water potential partially reflects soil water potential and thus also soil moisture. However, the relationship between soil moisture and soil water potential is highly nonlinear and strongly dependent on soil type (e.g., van Genuchten 1980), and stem water potential also reflects the sap flux and the hydraulic conductance in series between the soil and stem. Furthermore, stem water potentials depend on tree-size (Ryan and Yoder 1997), stomatal regulation (i.e., isohydricity; Woodruff et al. 2015) and plant water storage, all of which cannot be captured from soil moistures or soil water potentials alone. In short, these recent sink-limited schemes have greatly improved vegetation models; however, their formulations do not consider the plant hydraulics fundamental to TDGMs and their underlying physiological mechanisms. We explicitly considered the roles of plant hydraulics in our TDGM by coupling to THORP, a tree model of hydraulics and carbon allocation (Potkay et al. 2021). Nonetheless, our model or similarly simple TDGMs could be easily coupled to any plant hydraulics scheme such as recently developed hydraulics schemes for DGVMs (Christoffersen et al. 2016, Eller et al. 2020, Li et al. 2021, Sabot et al. 2020).

## Supplementary data

Supplementary data for this article are available at *Tree Physiology* online.

## Acknowledgments

We are grateful to Drs Kathy Steppe, Michael Ryan, Maurizio Mencuccini and an anonymous reviewer for their suggestions and insights to improve the manuscript.

#### Authors' contributions

A.P. designed, coded and ran the models. A.P., T.H., A.T.T. and Y.F. designed the simulation experiments. A.P. led the writing. A.P., T.H., A.T.T. and Y.F. analyzed data and contributed to interpretation, discussion and the final version.

## Conflict of interest

None declared.

## **Funding**

A.P. and Y. F. acknowledges the support of CUAHSI Path Finder travel grant and National Science Foundation grants (EAR-1528298, AGS-1852707).

#### References

- von Allmen EI, Sperry JS, Smith DD, Savage VM, Enquist BJ, Reich PB, Bentley LP (2012) A species-level model for metabolic scaling of trees II. Testing in a ring-and diffuse-porous species. Funct Ecol 26:1066–1076.
- Babst F, Bodesheim P, Charney N, Friend AD, Girardin MP, Klesse S, Evans ME (2018) When tree rings go global: challenges and opportunities for retro-and prospective insight. Quat Sci Rev 197:1–20.
- Ballantyne AP, Andres R, Houghton R, Stocker BD, Wanninkhof R, Anderegg W, Alden C (2015) Audit of the global carbon budget: estimate errors and their impact on uptake uncertainty. Biogeosciences 12:2565–2584.
- Bartlett MK, Scoffoni C, Sack L (2012) The determinants of leaf turgor loss point and prediction of drought tolerance of species and biomes: a global meta-analysis. Ecol Lett 15:393–405.
- Bartlett MK, Zhang Y, Kreidler N, Sun S, Ardy R, Cao K, Sack L (2014) Global analysis of plasticity in turgor loss point, a key drought tolerance trait. Ecol Lett 17:1580–1590.
- Bentley LP, Stegen JC, Savage VM, Smith DD, von Allmen EI, Sperry JS, Enquist BJ (2013) An empirical assessment of tree branching networks and implications for plant allometric scaling models. Ecol Lett 16:1069–1078.
- Bouchard C, Granjean BP (1995) A neural network correlation for the variation of viscosity of sucrose aqueous solutions with temperature and concentration. LWT-Food Sci Technol 28:157–159.
- Bravo F, Montero G (2001) Site index estimation in scots pine (*Pinus sylvestris* L.) stands in the high Ebro Basin (northern Spain) using soil attributes. Forestry 74:395–406.
- Buckley TN, Roberts DW (2006) DESPOT, a process-based tree growth model that allocates carbon to maximize carbon gain. Tree Physiol 26:129–144.
- Cabon A, Fernández-de-Uña L, Gea-Izquierdo G, Meinzer FC, Woodruff DR, Martínez-Vilalta J, De Cáceres M (2020) Water potential control of turgor-driven tracheid enlargement in Scots pine at its xeric distribution edge. New Phytol 225:209–221.
- Cabon A, Peters RL, Fonti P, Martínez-Vilalta J, De Cáceres M (2020) Temperature and water potential co-limit stem cambial activity along a steep elevational gradient. New Phytol 226:1325–1340.
- Cannell MG (1982) World forest biomass and primary production data. Academic Press, London.
- Chan T, Hölttä T, Berninger F, Mäkinen H, Nöjd P, Mencuccini M, Nikinmaa E (2016) Separating water-potential induced swelling and shrinking from measured radial stem variations reveals a cambial growth and osmotic concentration signal. Plant Cell Environ 39:233–244.
- Christoffersen BO, Gloor M, Fauset S, Fyllas NM, Galbraith DR, Baker TR, Sevanto S (2016) Linking hydraulic traits to tropical forest function in a size-structured and trait-driven model (TFS v. 1-hydro). Geosci Model Dev 9:4227–4255.
- Chung HH, Barnes RL (1977) Photosynthate allocation in *Pinus taeda taeda*. I. Substrate requirements for synthesis of shoot biomass. Can J For Res 7:106–111.
- Clerx LE, Rockwell FE, Savage JA, Holbrook NM (2020) Ontogenetic scaling of phloem sieve tube anatomy and hydraulic resistance with tree height in *Quercus rubra*. Am J Bot 107:852–863.
- Cook ER, Briffa KR, Shiyatov S, Mazepa V (1990) Tree-ring standardization and growth-trend estimation. In: Cook ER, Kairiukstis L (eds) Methods of dendrochronology: applications in the environmental sciences. Kluwer Academic Publishers, Dordrecht, The Netherlands, pp. 104–123.
- Coomes DA, Allen RB (2009) Testing the metabolic scaling theory of tree growth. J Ecol 97:1369–1373.

- Coomes DA, Lines ER, Allen RB (2011) Moving on from metabolic scaling theory: hierarchical models of tree growth and asymmetric competition for light. J Ecol 99:748–756.
- Cosgrove DJ (1997) Relaxation in a high-stress environment: the molecular bases of extensible cell walls and cell enlargement. Plant Cell 9:1031.
- Coussement J, De Swaef T, Lootens P, Steppe K (2020) Turgor-driven plant growth applied in a soybean functional-structural plant model. Ann Bot 126: 729–744.
- Dannoura M, Epron D, Desalme D, Massonnet C, Tsuji S, Plain C, Gérant D (2019) The impact of prolonged drought on phloem anatomy and phloem transport in young beech trees. Tree Physiol 39: 201–210.
- Daudet FA, Lacointe A, Gaudillere JP, Cruiziat P (2002) Generalized Münch coupling between sugar and water fluxes for modelling carbon allocation as affected by water status. J Theor Biol 214:481–498.
- De Pury DGG, Farquhar GD (1997) Simple scaling of photosynthesis from leaves to canopies without the errors of big-leaf models. Plant Cell Environ 20:537–557.
- De Schepper V, Steppe K (2010) Development and verification of a water and sugar transport model using measured stem diameter variations. J Exp Bot 61:2083–2099.
- Dewar RC (1993) A root-shoot partitioning model based on carbonnitrogen-water interactions and munch phloem flow. Funct Ecol 7:356–368.
- Dietrich L, Hoch G, Kahmen A, Körner C (2018) Losing half the conductive area hardly impacts the water status of mature trees. Sci Rep 8:1–9.
- Dietze MC, Sala A, Carbone MS, Czimczik CI, Mantooth JA, Richardson AD, Vargas R (2014) Nonstructural carbon in woody plants. Annu Rev Plant Biol 65:667–687.
- Eckes-Shephard AH, Tiavlovsky E, Chen Y, Fonti P, Friend AD (2021) Direct response of tree growth to soil water and its implications for terrestrial carbon cycle modelling. Glob Chang Biol 27: 121–135.
- Eller CB, Rowland L, Mencuccini M, Rosas T, Williams K, Harper A, Oliveira RS (2020) Stomatal optimization based on xylem hydraulics (SOX) improves land surface model simulation of vegetation responses to climate. New Phytol 226:1622–1637.
- Enquist BJ, Niklas KJ (2002) Global allocation rules for patterns of biomass partitioning in seed plants. Science 295:1517–1520.
- Enquist BJ, West GB, Charnov EL, Brown JH (1999) Allometric scaling of production and life-history variation in vascular plants. Nature 401:907–911.
- Epron D, Dannoura M, Ishida A, Kosugi Y (2019) Estimation of phloem carbon translocation belowground at stand level in a hinoki cypress stand. Tree Physiol 39:320–331.
- Farquhar GD, von Caemmerer SV, Berry JA (1980) A biochemical model of photosynthetic CO 2 assimilation in leaves of C 3 species. Planta 149:78–90.
- Fatichi S, Leuzinger S, Körner C (2014) Moving beyond photosynthesis: from carbon source to sink-driven vegetation modeling. New Phytol 201:1086–1095.
- Fatichi S, Pappas C, Zscheischler J, Leuzinger S (2019) Modelling carbon sources and sinks in terrestrial vegetation. New Phytol 221:652–668.
- Frensch J, Hsiao TC (1995) Rapid response of the yield threshold and turgor regulation during adjustment of root growth to water stress in Zea mays. Plant Physiol 108:303–312.
- Friedlingstein P (2015) Carbon cycle feedbacks and future climate change. Philos Trans A Math Phys Eng Sci 373:20140421.
- Friend AD, Eckes-Shephard AH, Fonti P, Rademacher TT, Rathgeber CB, Richardson AD, Turton RH (2019) On the need to consider wood

- formation processes in global vegetation models and a suggested approach. Ann For Sci 76:1–13.
- Fritts H (1976) Tree rings and climate. Academic Press, New York, NY, LISA
- Fritts HC, Vaganov EA, Sviderskaya IV, Shashkin AV (1991) Climatic variation and tree-ring structure in conifers: empirical and mechanistic models of tree-ring width, number of cells, cell size, cell-wall thickness and wood density. Climate Res 1:97–116.
- Fu X, Meinzer FC (2019) Metrics and proxies for stringency of regulation of plant water status (iso/anisohydry): a global data set reveals coordination and trade-offs among water transport traits. Tree Physiol 39:122–134.
- Gazol A, Camarero JJ, Anderegg WRL, Vicente-Serrano SM (2017) Impacts of droughts on the growth resilience of northern hemisphere forests. Glob Ecol Biogeogr 26:166–176.
- Génard M, Fishman S, Vercambre G, Huguet JG, Bussi C, Besset J, Habib R (2001) A biophysical analysis of stem and root diameter variations in woody plants. Plant Physiol 126:188–202.
- van Genuchten MT (1980) A closed-form equation for predicting the hydraulic conductivity of unsaturated soils. Soil Sci Soc Am J 44:892–898.
- Gifford RM, Evans LT (1981) Photosynthesis, carbon partitioning, and yield. Annu Rev Plant Physiol 32:485–509.
- Givnish TJ, Wong SC, Stuart-Williams H, Holloway-Phillips M, Farquhar GD (2014) Determinants of maximum tree height in Eucalyptus species along a rainfall gradient in Victoria, Australia. Ecology 95:2991–3007.
- Green PB, Erickson RO, Buggy J (1971) Metabolic and physical control of cell elongation rate: in vivo studies in Nitella. Plant Physiology 47(3):423–430.
- Guillemot J, Francois C, Hmimina G, Dufrêne E, Martin-StPaul NK, Soudani K, Delpierre N (2017) Environmental control of carbon allocation matters for modelling forest growth. New Phytol 214:180–193.
- Hall AJ, Minchin PEH (2013) A closed-form solution for steady-state coupled phloem/xylem flow using the Lambert-W function. Plant Cell Environ 36:2150–2162.
- Hayat A, Hacket-Pain AJ, Pretzsch H, Rademacher TT, Friend AD (2017) Modeling tree growth taking into account carbon source and sink limitations. Front Plant Sci 8:182.
- Hölttä T, Kurppa M, Nikinmaa E (2013) Scaling of xylem and phloemtransport capacity and resource usage with tree size. Front Plant Sci 4:496.
- Hölttä T, Mäkinen H, Nöjd P, Mäkelä A, Nikinmaa E (2010) A physiological model of softwood cambial growth. Tree Physiol 30:1235–1252.
- Hölttä T, Mencuccini M, Nikinmaa E (2009) Linking phloem function to structure: analysis with a coupled xylem-phloem-transport model. J Theor Biol 259:325–337.
- Hölttä T, Vesala T, Sevanto S, Perämäki M, Nikinmaa E (2006) Modeling xylem and phloem water flows in trees according to cohesion theory and Münch hypothesis. Trees 20:67–78.
- Huang H, Ran J, Ji M, Wang Z, Dong L, Hu W, Deng J (2020) Water content quantitatively affects metabolic rates over the course of plant ontogeny. New Phytol 228:1524–1534.
- IPCC (2019) IPCC Working group III Technical Support Unit, Imperial College, "Desertification," in Climate Change and Land: an IPCC special report on climate change, desertification, land degradation, sustainable land management, food security, and greenhouse gas fluxes in terrestrial ecosystems. IPCC Working group III Technical Support Unit, Imperial College, London, UK, pp. 1–174.
- Jensen KH, Berg-Sørensen K, Friis SM, Bohr T (2012) Analytic solutions and universal properties of sugar loading models in Münch phloem flow. J Theor Biol 304:286–296.

- Jensen KH, Savage JA, Holbrook NM (2013) Optimal concentration for sugar transport in plants. J R Soc Interface 10:20130055.
- Jones MM, Turner NC (1978) Osmotic adjustment in leaves of Sorghum in response to water defecits. Plant Physiol 61:122–126.
- Jones S, Rowland L, Cox P, Hemming D, Wiltshire A, Williams K, Mencuccini M (2019) The impact of a simple representation of nonstructural carbohydrates on the simulated response of tropical forests to drought. Biogeosci 17:1–26.
- Jyske T, Hölttä T (2015) Comparison of phloem and xylem hydraulic architecture in *Picea abies* stems. New Phytol 205:102–115.
- Kalnay E, Kanamitsu M, Kistler R, Collins W, Deaven D, Gandin L, Zhu Y (1996) The NCEP/NCAR 40-year reanalysis project. Bull Am Meteorol Soc 77:437–472.
- Kempes CP, West GB, Crowell K, Girvan M (2011) Predicting maximum tree heights and other traits from allometric scaling and resource limitations. PLoS One 6(6):e20551.
- King DA (1990) The adaptive significance of tree height. Am Nat 135:809–828.
- Kira T (1978) Community architecture and organic matter dynamics in tropical lowland rain forests of Southeast Asia with special reference to Pasoh forest, West Malaysia. In: Tomlinson PB, Zimmermann MH (eds) Tropical Trees as Living Systems, Cambridge University Press, Cambridge, pp. 561–590.
- Kirkham MB, Gardner WR, Gerloff GC (1972) Regulation of cell division and cell enlargement by turgor pressure. Plant Physiol 49:961–962.
- Knoblauch M, Knoblauch J, Mullendore DL, Savage JA, Babst BA, Beecher SD, Holbrook NM (2016) Testing the Münch hypothesis of long distance phloem transport in plants. Elife 5:e15341.
- Knoblauch M, Oparka K (2012) The structure of the phloem–still more questions than answers. Plant J 70:147–156.
- Knoblauch M, Peters WS (2017) What actually is the Münch hypothesis? A short history of assimilate transport by mass flow. J Integr Plant Biol 59:292–310.
- Koch GW, Sillett SC, Jennings GM, Davis SD (2004) The limits to tree height. Nature 428:851–854.
- Körner C (2003) Carbon limitation in trees. J Ecol 91:4-17.
- Körner C (2015) Paradigm shift in plant growth control. Curr Opin Plant Biol 25:107–114.
- Lazzarin M, Zweifel R, Anten N, Sterck FJ (2019) Does phloem osmolality affect diurnal diameter changes of twigs but not of stems in scots pine? Tree Physiol 39:275–283.
- Le Quéré C, Andrew RM, Friedlingstein P, Sitch S, Pongratz J, Manning AC, Boden TA (2018) Global carbon budget 2017. Earth System Science Data Discussions, pp. 1–79.
- Lemoine R, La Camera S, Atanassova R, Dédaldéchamp F, Allario T, Pourtau N, Durand M (2013) Source-to-sink transport of sugar and regulation by environmental factors. Front Plant Sci 4:272.
- Lempereur M, Martin-StPaul NK, Damesin C, Joffre R, Ourcival JM, Rocheteau A, Rambal S (2015) Growth duration is a better predictor of stem increment than carbon supply in a Mediterranean oak forest: implications for assessing forest productivity under climate change. New Phytol 207:579–590.
- Leuzinger S, Manusch C, Bugmann H, Wolf A (2013) A sink-limited growth model improves biomass estimation along boreal and alpine tree lines. Glob Ecol Biogeogr 22:924–932.
- Li HT, Han XG, Wi JG (2005) Lack of evidence for 3/4 scaling of metabolism in terrestrial plants. J Integr Plant Biol 47:1173–1183.
- Li L, Yang ZL, Matheny AM, Zheng H, Swenson SC, Lawrence DM, Leung LR (2021) Representation of plant hydraulics in the Noah-MP land surface model: model development and multi-scale evaluation. J Adv Model Earth Syst 13: e2020MS002214.
- Liesche J, Pace MR, Xu Q, Li Y, Chen S (2017) Height-related scaling of phloem anatomy and the evolution of sieve element end wall types in woody plants. New Phytol 214:245–256.

- Lockhart JA (1965) An analysis of irreversible plant cell elongation. J Theor Biol 8:264–275.
- Losada JM, Holbrook NM (2019) Scaling of phloem hydraulic resistance in stems and leaves of the understory angiosperm shrub *Illicium parviflorum*. Am J Bot 106:244–259.
- Mäkelä A (1985) Differential games in evolutionary theory: height growth strategies of trees. Theor Popul Biol 27:239–267.
- Mäkelä A (1986) Implications of the pipe model theory on dry matter partitioning and height growth in trees. J Theor Biol 123: 103–120.
- Mäkelä A, Grönlund L, Schiestl-Aalto P, Kalliokoski T, Hölttä T (2019) Current-year shoot hydraulic structure in two boreal conifers—implications of growth habit on water potential. Tree Physiol 39:1995–2007.
- Marshall JD, Monserud RA (2003) Foliage height influences specific leaf area of three conifer species. Can J For Res 33:164–170.
- Martínez-Vilalta J, Poyatos R, Aguadé D, Retana J, Mencuccini M (2014) A new look at water transport regulation in plants. New Phytol 204:105–115.
- McMahon TA (1973) Size and shape in biology. Science 179: 1201–1204.
- Meinzer FC, Woodruff DR, Marias DE, Smith DD, McCulloh KA, Howard AR, Magedman AL (2016) Mapping 'hydroscapes' along the iso-to anisohydric continuum of stomatal regulation of plant water status. Ecol Lett 19:1343–1352.
- Mencuccini M, Grace J (1996) Hydraulic conductance, light interception and needle nutrient concentration in Scots pine stands and their relations with net primary productivity. Tree Physiol 16:459–468.
- Mencuccini M, Salmon Y, Mitchell P, Hölttä T, Choat B, Meir P, Pfautsch S (2017) An empirical method that separates irreversible stem radial growth from bark water content changes in trees: theory and case studies. Plant Cell Environ 40:290–303.
- Millard P, Sommerkorn M, Grelet GA (2007) Environmental change and carbon limitation in trees: a biochemical, ecophysiological and ecosystem appraisal. New Phytol 175:11–28.
- Mina M, Martin-Benito D, Bugmann H, Cailleret M (2016) Forward modeling of tree-ring width improves simulation of forest growth responses to drought. Agric For Meteorol 221:13–33.
- Mori S, Yamaji K, Ishida A, Prokushkin SG, Masyagina OV, Hagihara A, Umari M (2010) Mixed-power scaling of whole-plant respiration from seedlings to giant trees. Proc Natl Acad Sci 107:1447–1451.
- Muller B, Pantin F, Génard M, Turc O, Freixes S, Piques M, Gibon Y (2011) Water deficits uncouple growth from photosynthesis, increase C content, and modify the relationships between C and growth in sink organs. J Exp Bot 62:1715–1729.
- Muller-Landau HC, Condit RS, Chave J, Thomas SC, Bohlman SA, Bunyavejchewin S, Ashton P (2006) Testing metabolic ecology theory for allometric scaling of tree size, growth and mortality in tropical forests. Ecol Lett 9:575–588.
- Münch E (1930) Die Stoffbewegungen in der Pflanze. Gustav Fischer, Jena.
- Nakahori K, Katou K, Okamoto H (1991) Auxin changes both the extensibility and the yield threshold of the cell wall of *Vigna hypocotyls*. Plant Cell Physiol 32:121–129.
- Niinemets U (1999) Components of leaf dry mass per area—thickness and density—alter photosynthetic capacity in reverse directions in woody plants. New Phytol 144:35–47.
- Nikinmaa E, Sievänen R, Hölttä T (2014) Dynamics of leaf gas exchange, xylem and phloem transport, water potential and carbohydrate concentration in a realistic 3-D model tree crown. Ann Bot 114:653–666.
- Niklas KJ, Enquist BJ (2001) Invariant scaling relationships for interspecific plant biomass production rates and body size. Proc Natl Acad Sci 98:2922–2927.

- Niklas KJ, Spatz HC (2004) Growth and hydraulic (not mechanical) constraints govern the scaling of tree height and mass. Proc Natl Acad Sci 101:15661–15663.
- Olson ME, Soriano D, Rosell JA, Anfodillo T, Donoghue MJ, Edwards EJ, Méndez-Alonzo R (2018) Plant height and hydraulic vulnerability to drought and cold. Proc Natl Acad Sci 115:7551–7556.
- Palahi M, Tomé M, Pukkala T, Trasobares A, Montero G (2004) Site index model for *Pinus sylvestris* in north-east Spain. For Ecol Manage 187:35–47.
- Paljakka T, Jyske T, Lintunen A, Aaltonen H, Nikinmaa E, Hölttä T (2017) Gradients and dynamics of inner bark and needle osmotic potentials in scots pine (*Pinus sylvestris L.*) and Norway spruce (*Picea abies L. karst*). Plant Cell Environ 40:2160–2173.
- Patrick JW (2013) Does Don Fisher's high-pressure manifold model account for phloem-transport and resource partitioning? Front Plant Sci 4:184.
- Paul MJ, Foyer CH (2001) Sink regulation of photosynthesis. J Exp Bot 52:1383–1400.
- Peng Y, Niklas KJ, Reich PB, Sun S (2010) Ontogenetic shift in the scaling of dark respiration with whole-plant mass in seven shrub species. Funct Ecol 24:502–512.
- Peters RL, Steppe K, Cuny HE, De Pauw DJ, Frank DC, Schaub M, Fonti P (2021) Turgor–a limiting factor for radial growth in mature conifers along an elevational gradient. New Phytol 229:213–229.
- Poorter H, Niklas KJ, Reich PB, Oleksyn J, Poot P, Mommer L (2012) Biomass allocation to leaves, stems and roots: meta-analyses of interspecific variation and environmental control. New Phytol 193: 30–50.
- Potkay A, Trugman A, Wang Y, Venturas MD, Anderegg WRL, Mattos CR, Fan Y (2021) Coupled whole-tree optimality and xylem-hydraulics explain dynamic biomass partitioning. New Phytol 230:2226–2245.
- Price CA, Ogle K, White EP, Weitz JS (2009) Evaluating scaling models in biology using hierarchical Bayesian approaches. Ecol Lett 12:641–651.
- Pritchard J, WYN Jones RG, Tomos AD (1990) Measurement of yield threshold and cell wal extensibility of intact wheat roots under different ionic, osmotic and temperature treatments. J Exp Bot 41:669–675.
- Reich PB, Tjoelker MG, Machado JL, Oleksyn J (2006) Universal scaling of respiratory metabolism, size and nitrogen in plants. Nature 439:457–461.
- Rosell JA (2016) Bark thickness across the angiosperms: more than just fire. New Phytol 211:90–102.
- Rosell JA, Olson ME, Anfodillo T, Martínez-Méndez N (2017) Exploring the bark thickness-stem diameter relationship: clues from lianas, successive cambia, monocots and gymnosperms. New Phytol 215:569–581.
- Ruehr NK, Offermann CA, Gessler A, Winkler JB, Ferrio JP, Buchmann N, Barnard RL (2009) Drought effects on allocation of recent carbon: from beech leaves to soil CO2 efflux. New Phytol 184:950–961.
- Russo SE, Wiser SK, Coomes DA (2007) Growth–size scaling relationships of woody plant species differ from predictions of the metabolic ecology model. Ecol Lett 10:889–901.
- Ryan MG, Phillips N, Bond BJ (2006) The hydraulic limitation hypothesis revisited. Plant Cell Environ 29:367–381.
- Ryan MG, Yoder BJ (1997) Hydraulic limits to tree height and tree growth. Bioscience 47:235–242.
- Sabot ME, De Kauwe MG, Pitman AJ, Medlyn BE, Verhoef A, Ukkola AM, Abramowitz G (2020) Plant profit maximization improves predictions of European forest responses to drought. New Phytol 226:1638–1655.

- Salmon Y, Dietrich L, Sevanto S, Hölttä T, Dannoura M, Epron D (2019) Drought impacts on tree phloem: from cell-level responses to ecological significance. Tree Physiol 39:173–191.
- Salmon Y, Lintunen A, Dayet A, Chan T, Dewar R, Vesala T, Hölttä T (2020) Leaf carbon and water status control stomatal and nonstomatal limitations of photosynthesis in trees. New Phytol 226:690–703.
- Salomón RL, De LR, Oleksyn J, De DP, Steppe K (2019) TReSpirea biophysical tree stem respiration model. New Phytol 225:2214— 2230.
- Savage JA, Beecher SD, Clerx L, Gersony JT, Knoblauch J, Losada JM, Holbrook NM (2017) Maintenance of carbohydrate transport in tall trees. Nat Plants 3:965–972.
- Savage VM, Bentley LP, Enquist BJ, Sperry JS, Smith DD, Reich PB, Von Allmen EI (2010) Hydraulic trade-offs and space filling enable better predictions of vascular structure and function in plants. Proc Natl Acad Sci 107:22722–22727.
- Saveyn A, Steppe K, Lemeur R (2007) Daytime depression in tree stem CO 2 efflux rates: is it caused by low stem turgor pressure? Ann Bot 99:477–485.
- Schiestl-Aalto P, Kulmala L, Mäkinen H, Nikinmaa E, Mäkelä A (2015) CASSIA–a dynamic model for predicting intra-annual sink demand and interannual growth variation in Scots pine. New Phytol 206:647–659.
- Schiestl-Aalto P, Ryhti K, Mäkelä A, Peltoniemi M, Bäck J, Kulmala L (2019) Analysis of the NSC storage dynamics in tree organs reveals the allocation to belowground symbionts in the framework of whole tree carbon balance. Front For Glob Change 2:17.
- Seleznyova AN, Hanan J (2017) Carbon transport revisited: a novel approach for solving quasi-stationary carbon transport in a system with Michaelis-Menten sources and sinks. Acta Horticulture 1160:269–276.
- Seleznyova AN, Hanan J (2018) Mechanistic modelling of coupled phloem/xylem transport for L-systems: combining analytical and computational methods. Ann Bot 121:991–1003.
- Sevanto S (2014) Phloem transport and drought. J Exp Bot 65:1751–1759.
- Sheil D, Salim A, Chave J, Vanclay J, Hawthorne WD (2006) Illumination-size relationships of 109 coexisting tropical forest tree species. J Ecol 94:494–507.
- Shinozaki K, Yoda K, Hozumi K, Kira T (1964) A quantitative analysis of plant form-the pipe model theory: I. Basic analyses. Japanese J Ecol 14:97–105.
- Simard S, Giovannelli A, Treydte K, Traversi ML, King GM, Frank D, Fonti P (2013) Intra-annual dynamics of non-structural carbohydrates in the cambium of mature conifer trees reflects radial growth demands. Tree Physiol 33:913–923.
- Smith DD, Sperry JS (2014) Coordination between water transport capacity, biomass growth, metabolic scaling and species stature in cooccurring shrub and tree species. Plant Cell Environ 37:2679–2690.
- Sperry JS, Adler FR, Campbell GS, Comstock JP (1998) Limitation of plant water use by rhizosphere and xylem conductance: results from a model. Plant Cell Environ 21:347–359.
- Sperry JS, Smith DD, Savage VM, Enquist BJ, McCulloh KA, Reich PB, von Allmen EI (2012) A species-level model for metabolic scaling in trees I. Exploring boundaries to scaling space within and across species. Funct Ecol 26:1054–1065.
- Sperry JS, Venturas MD, Anderegg WR, Mencuccini M, Mackay DS, Wang Y, Love DM (2017) Predicting stomatal responses to the environment from the optimization of photosynthetic gain and hydraulic cost. Plant Cell Environ 40:816–830.
- Steppe K, De Pauw DJ, Lemeur R (2008) Validation of a dynamic stem diameter variation model and the resulting seasonal changes in calibrated parameter values. Ecol Model 218:247–259.

- Steppe K, De Pauw DJ, Lemeur R, Vanrolleghem PA (2006) A mathematical model linking tree sap flow dynamics to daily stem diameter fluctuations and radial stem growth. Tree Physiol 26:257–273.
- Steppe K, Sterck F, Deslauriers A (2015) Diel growth dynamics in tree stems: linking anatomy and ecophysiology. Trends Plant Sci 20:335–343.
- Tao S, Guo Q, Li C, Wang Z, Fang J (2016) Global patterns and determinants of forest canopy height. Ecology 97:3265–3270.
- Thompson MV, Holbrook NM (2003*a*) Application of a single-solute non-steady-state phloem model to the study of long-distance assimilate transport. J Theor Biol 220:419–455.
- Thompson MV, Holbrook NM (2003b) Scaling phloem-transport: water potential equilibrium and osmoregulatory flow. Plant Cell Environ 26:1561–1577.
- Thompson MV, Holbrook NM (2004) Scaling phloem-transport: information transmission. Plant Cell Environ 27:509–519.
- Thornley JHM (1972) A balanced quantitative model for root: shoot ratios in vegetative plants. Ann Bot 36:431–441.
- Vaganov EA, Hughes MK, Shashkin AV (2006) Growth dynamics of conifer tree rings: images of past and future environments, Vol. 183. Springer, New York.
- Venturas MD, Sperry JS, Hacke UG (2017) Plant xylem hydraulics: what we understand, current research, and future challenges. J Integr Plant Biol 59:356–389.
- Venturas MD, Sperry JS, Love DM, Frehner EH, Allred MG, Wang Y, Anderegg WR (2018) A stomatal control model based on optimization of carbon gain versus hydraulic risk predicts aspen sapling responses to drought. New Phytol 220:836–850.
- Venturas MD, Todd HN, Trugman AT, Anderegg WR (2020) Understanding and predicting forest mortality in the western United States using long-term forest inventory data and modeled hydraulic damage. New Phytol 230:1896–1910.
- Wang Y, Sperry JS, Anderegg WR, Venturas MD, Trugman AT (2020) A theoretical and empirical assessment of stomatal optimization modeling. New Phytol 227:311–325.

- Wang Y, Sperry JS, Venturas MD, Trugman AT, Love DM, Anderegg WR (2019) The stomatal response to rising CO2 concentration and drought is predicted by a hydraulic trait-based optimization model. Tree Physiol 39:1416–1427.
- Waring RH, Schlesinger WH (1985) Forest ecosystems, analysis at multiples scales, Vol. 55. Academic Press, Orlando, FL.
- West GB, Brown JH, Enquist BJ (1999) A general model for the structure and allometry of plant vascular systems. Nature 400: 664–667.
- Wolf A, Ciais P, Bellassen V, Delbart N, Field CB, Berry JA (2011) Forest biomass allometry in global land surface models. Global Biogeochem Cycles 25:GB3015.
- Woodruff DR (2014) The impacts of water stress on phloem transport in Douglas-fir trees. Tree Physiol 34:5–14.
- Woodruff DR, Bond BJ, Meinzer FC (2004) Does turgor limit growth in tall trees? Plant Cell Environ 27:229–236.
- Woodruff DR, Meinzer FC (2011) Water stress, shoot growth and storage of non-structural carbohydrates along a tree height gradient in a tall conifer. Plant Cell Environ 34:1920–1930.
- Woodruff DR, Meinzer FC, Marias DE, Sevanto S, Jenkins MW, McDowell NG (2015) Linking nonstructural carbohydrate dynamics to gas exchange and leaf hydraulic behavior in *Pinus edulis* and *Juniperus monosperma*. New Phytol 206:411–421.
- Wyckoff PH, Clark JS (2005) Tree growth prediction using size and exposed crown area. Can J For Res 35:13–20.
- Xia J, Yuan W, Lienert S, Joos F, Ciais P, Viovy N, Tian X (2019) Global patterns in net primary production allocation regulated by environmental conditions and forest stand age: a model-data comparison. J Geophys Res Biogeo 124: 2039–2059.
- Zhu SD, Chen YJ, Ye Q, He PC, Liu H, Li RH, Cao KF (2018) Leaf turgor loss point is correlated with drought tolerance and leaf carbon economics traits. Tree Physiol 38:658–663.
- Zweifel R, Sterck F, Braun S, Buchmann N, Eugster W, Gessler A, Etzold S (2021) Why trees grow at night. New Phytol 231:2174–2185.